Molecular Cell
Article

Misfolded Membrane Proteins Are Specifically Recognized by the Transmembrane Domain of the Hrd1p Ubiquitin Ligase

Brian K. Sato,[1] Daniel Schulz,[1] Phong H. Do,[1] and Randolph Y. Hampton[1,*]
[1]Section of Cell and Developmental Biology, Division of Biological Sciences, University of California, San Diego, 9500 Gilman Drive, La Jolla, CA 92093, USA
*Correspondence: rhampton@ucsd.edu
DOI 10.1016/j.molcel.2009.03.010

SUMMARY

Quality control pathways such as ER-associated degradation (ERAD) employ a small number of factors to specifically recognize a wide variety of protein substrates. Delineating the mechanisms of substrate selection is a principle goal in studying quality control. The Hrd1p ubiquitin ligase mediates ERAD of numerous misfolded proteins including soluble, lumenal ERAD-L and membrane-anchored ERAD-M substrates. We tested if the Hrd1p multispanning membrane domain was involved in ERAD-M specificity. In this work, we have identified site-directed membrane domain mutants of Hrd1p impaired only for ERAD-M and normal for ERAD-L. Furthermore, other Hrd1p variants were specifically deficient for degradation of individual ERAD-M substrates. Thus, the Hrd1p transmembrane region bears determinants of high specificity in the ERAD-M pathway. From in vitro and interaction studies, we suggest a model in which the Hrd1p membrane domain employs intramembrane residues to evaluate substrate misfolding, leading to selective ubiquitination of appropriate ERAD-M clients.

INTRODUCTION

The endoplasmic reticulum-associated degradation (ERAD) pathway mediates the destruction of numerous normal and misfolded ER-localized proteins (Hampton, 2002a; Hampton et al., 1996; Ravid et al., 2006). The ERAD pathway has been implicated in a wide variety of processes, including sterol synthesis, rheumatoid arthritis, fungal differentiation, cystic fibrosis, and several neurodegenerative diseases (Amano et al., 2003; Hampton and Rine, 1994; Liang et al., 2006; Swanson et al., 2001; Zhang et al., 2002). Accordingly, there is great impetus to understand the molecular mechanisms that mediate this important route of protein degradation.

ERAD proceeds by the ubiquitin-proteasome pathway, in which an ER-localized substrate is covalently modified by three enzymes in order to form a multiubiquitin chain that is recognized by the cytosolic 26S proteasome (Voges et al., 1999). The E1 ubiquitin-activating enzyme uses ATP to covalently activate and then add ubiquitin to an E2 ubiquitin-conjugating enzyme. Ubiquitin is then transferred from the ubiquitin-charged E2 to the substrate or the growing ubiquitin chain by the action of an E3 ubiquitin ligase, resulting in a substrate-attached multiubiquitin chain. In most cases, ancillary factors participate in substrate recognition and transfer of the ubiquitinated substrate to the proteasome (Carvalho et al., 2006; Denic et al., 2006; Richly et al., 2005).

The HRD pathway is one of the principal routes of ERAD in eukaryotes, being responsible for the degradation of both lumenal and membrane-bound misfolded ER proteins (Hampton et al., 1996; Knop et al., 1996; Vashist and Ng, 2004). The HRD pathway E3 ligase is the highly conserved Hrd1p, which is rate-limiting for degradation (Bays et al., 2001a). Hrd1p is a multispanning ER membrane protein, consisting of an N-terminal membrane anchor linked to a soluble C-terminal domain with a RING-H2 domain characteristic of many E3 ligases (Figure 1). The C-terminal region is responsible for catalyzing the transfer of ubiquitin from the appropriate E2s to ERAD substrates (Bays et al., 2001a). However, successful degradation of ERAD substrates requires the presence of the Hrd1p membrane anchor, either as the full-length protein or when expressed in *trans* with the active C-terminal region (Gardner et al., 2000). The multispanning Hrd1p membrane domain has numerous known functions, including binding to and communication with the lumenal domain of Hrd3p, correct placement of the C-terminal ligase domain, and recruitment of ERAD factors for recognition of misfolded proteins and for later steps in the pathway such as retrotranslocation (Bazirgan et al., 2006; Gardner et al., 2000; Neuber et al., 2005). The namesake substrate of the HRD pathway is Hmg2p, a yeast isozyme of the sterol pathway enzyme HMG-CoA reductase (HMGR). Hmg2p undergoes regulated entry into the HRD pathway so that when production of sterol pathway products is high, HRD-dependent degradation of Hmg2p is more rapid (Gardner and Hampton, 1999; Gardner et al., 2001a). Regulation of Hmg2 stability appears to occur by pathway signal-induced misfolding of Hmg2p that improves HRD pathway recognition (Gardner et al., 2001b). In this way, ERAD is employed as part of the feedback regulation of sterols, and a similar mechanism operates in mammals (Goldstein and Brown, 1990; Hampton, 2002b; Hampton and Garza, 2009).

HRD pathway substrates fall into two broad categories: soluble lumenal proteins such as CPY*, or integral membrane

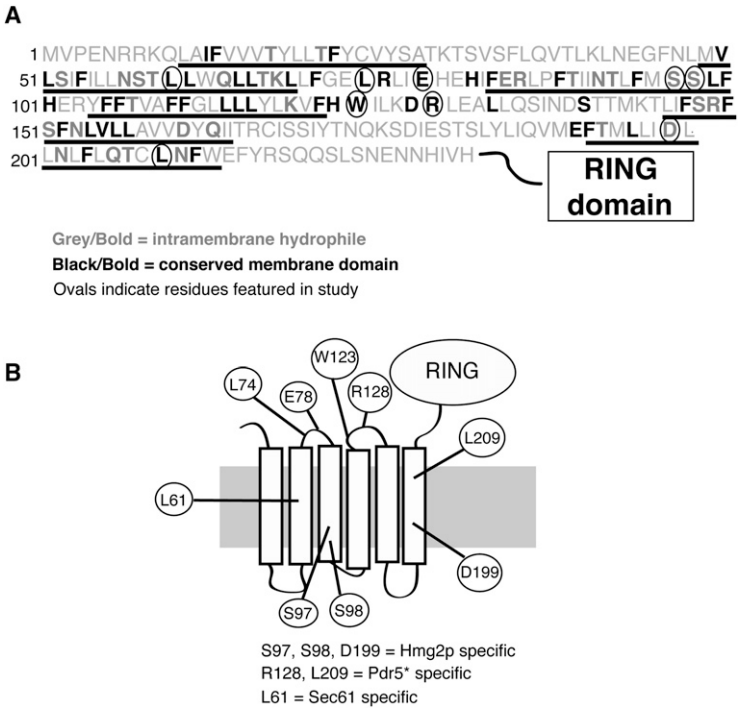

Figure 1. The Hrd1p Transmembrane Domain

(A) The amino acid sequence of the *HRD1* N-terminal transmembrane region. Underlined residues highlight the six transmembrane spans as defined by Deak and Wolf (2001). Residues in bold are those mutated to alanine in order to determine their role in Hrd1p-dependent degradation.

(B) The residues of interest discussed in the text.

proteins such as Hmg2p or Pdr5* (Hampton et al., 1996; Knop et al., 1996; Plemper et al., 1998). Substrates are diverse, indicating that misfolded proteins are recognized by structural criteria that transcend the absence of any primary sequence similarity between the various members of each group. In the case of lumenal proteins such as CPY*, a variety of factors have been proposed to mediate the recognition of hallmarks of misfolding required for presentation to the HRD machinery. The classic chaperone Kar2p, the lumenal lectins Htm1p and Yos9p, and the ER-anchored lumenal domain of Hrd3p have all been implicated in recognition of lumenal ERAD substrates (Carvalho et al., 2006; Denic et al., 2006; Jakob et al., 2001). However, neither Kar2p or Yos9p is required for degradation of membrane-bound substrates, nor is Hrd3p if sufficient Hrd1p is present (Gardner et al., 2000). Similarly, Der1p is required for lumenal substrate degradation but is dispensible for integral membrane substrates such as Hmg2p or Pdr5* (Plemper et al., 1998; Sato and Hampton, 2006).

Because of these distinctions between lumenal and membrane-anchored substrates, the degradation of each class of proteins has been referred to as ERAD-L for the lumenal substrate pathway and ERAD-M for the integral membrane pathway. In striking contrast to the success of identifying factors for recognition of ERAD-L substrates, little is known about how membrane proteins are recognized as ERAD substrates (Carvalho et al., 2006; Denic et al., 2006).

In many cases in the ubiquitin pathway, the E3 ubiquitin ligase is the primary mediator of substrate recognition. We wondered if the ubiquitin ligase Hrd1p plays this direct role in ERAD-M. Although less is known about what features an aberrant or ''misfolded'' membrane protein might possess, those features would likely be present within or near the bilayer. Thus, the multispanning transmembrane domain of Hrd1p would be the appropriate region to mediate recognition of ERAD-M substrates. One idea is that a correctly folded and assembled integral membrane protein would be expected to present no free hydrophilic groups within the lipid region of the membrane, while a misfolded membrane protein would expose hydrophobic groups to the bilayer, allowing detection by interacting with similar groups in an integral membrane E3. In fact, the Hrd1p transmembrane anchor has a high proportion of hydrophilic R groups in its six transmembrane spans that might serve such a detection function (Figure 1; Deak and Wolf, 2001).

As part of a systematic analysis of the Hrd1p transmembrane region, we have studied the effects of mutating these hydrophilic groups, along with other residues that are highly conserved in Hrd1p orthologs, to query the mechanisms of specific substrate recognition. We have identified mutants each deficient in recognition of distinct ERAD-M substrates, indicating a role for the membrane domain in substrate detection. Furthermore, a detailed analysis of one of our recognition-deficient mutants indicates a role for the transmembrane domain in regulation of the activity of the ligase upon encountering a misfolded substrate, consistent with our earlier studies on Hrd1p-substrate mechanisms. Thus, Hrd1p bears a code for detection of misfolded proteins in a membrane environment. Unraveling this code will have important implications in understanding the many processes that pertain to management of protein quality in normal and pathological cellular states.

RESULTS

The Hrd1p transmembrane region contains a large number of intrabilayer hydrophilic amino acids, which we targeted for mutation (Figure 1). We also compared the sequence of the *Saccharomyces cerevisiae* transmembrane region to that of human Hrd1, human gp78, *Schizosaccharomyces pombe* Hrd1, and *Yarrowia lipolytica* Hrd1 to identify conserved residues, as they might be expected to have key roles in Hrd1 action. In total, 77 distinct Hrd1 mutants were created in which a single amino acid codon was changed to alanine. In some cases, tandem codons were altered to two alanines. If Hrd1p participated in the specific detection of substrates, we reasoned it should be possible to find mutants deficient in degradation of distinct classes of substrates, or perhaps even deficient in degradation of individual substrates. In contrast, the C399S RING mutant is unable to degrade all ERAD substrates (Bays et al., 2001a; see below).

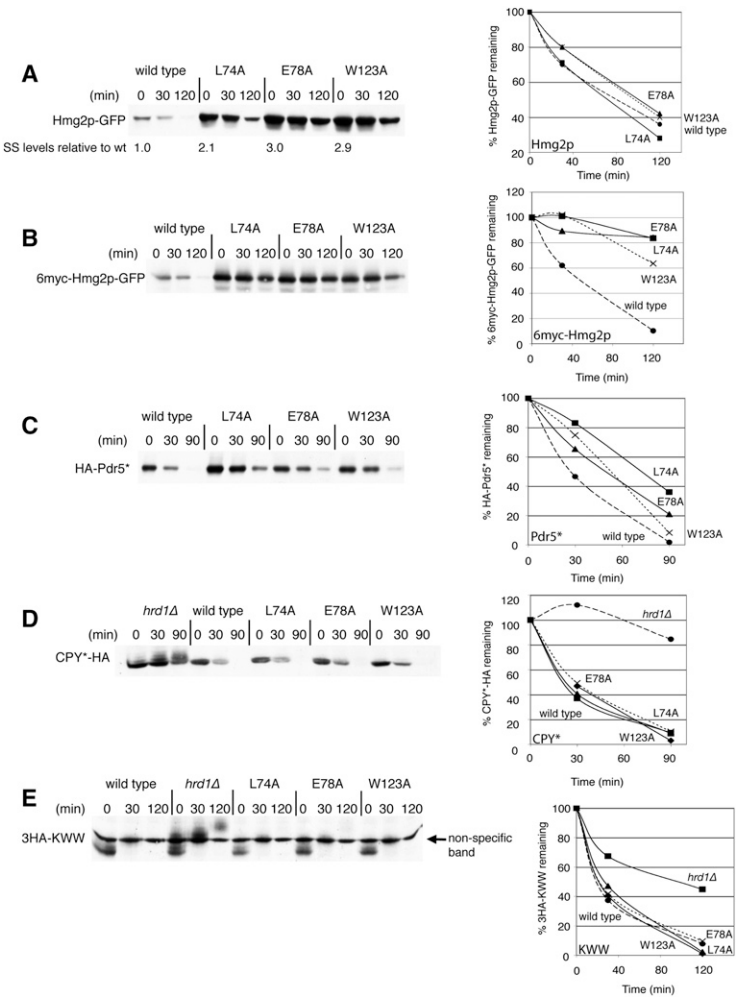

Figure 2. Amino Acids L74, E78, and W123 in Hrd1p Were Important for the Degradation of ERAD-M Substrates

(A–E) Degradation of each tagged ERAD substrate was measured by cycloheximide chase in isogenic strains. Each *hrd1*Δ strain was transformed with the indicated version of *HRD1* or empty vector for *hrd1*Δ. Total protein levels in each lane were equal as verified by India ink staining (data not shown). Steady-state Hmg2p-GFP protein (SS levels) was measured at t = 0 for each mutant strain and compared to wild-type Hrd1p-expressing cells. For (A), Hmg2p degradation was quantified using flow cytometry. Each point on the graph is the mean fluorescence of 10,000 cells with a standard error of the mean of ± 1%. For non-GFP-tagged substrates (B–E), statistics were taken from the adjacent western blot (a representative experiment) quantified with a Typhoon 9400 and ImageQuant 5.2.

We tested each Hrd1p mutant to evaluate the altered residue's importance in Hrd1p-dependent ERAD. Specifically, we evaluated ERAD-M, ERAD-L, and Hrd1p self-catalyzed degradation, since all three modes of HRD-dependent degradation have distinct rules and requirements (Carvalho et al., 2006; Gardner et al., 2000; Vashist and Ng, 2004). To assess ERAD-M, we tested the degradation of the integral ER membrane protein Hmg2p by each Hrd1p variant. We used a noncatalytic Hmg2p-GFP, which allows evaluation of protein stability by flow cytometry or immunoblotting (Gardner and Hampton, 1999). To evaluate ERAD-L, each Hrd1p mutant was screened with KWW (Vashist and Ng, 2004). KWW is an engineered substrate with a misfolded lumenal domain that enters the HRD pathway by ERAD-L. To evaluate Hrd1p self-degradation, we expressed each in a *hrd3*Δ null strain. In the absence of Hrd3p, Hrd1p undergoes extremely rapid degradation catalyzed by its own RING domain (Gardner et al., 2000). This self-degradation has been posited to be important for Hrd1p regulation, and appears to be distinct from both ERAD-L and ERAD-M (S. Carroll and R.Y.H., unpublished data). Thus, to test these aspects of Hrd1p function, each individual Hrd1p mutant was transformed into *hrd1*Δ strains expressing either Hmg2p-GFP or KWW, or a *hrd3*Δ strain, allowing examination of the mutant's effects on ERAD-M, ERAD-L, and Hrd1p self-degradation, respectively. The effect of each Hrd1p mutant on substrate stability was assayed by cycloheximide chase in which log phase cultures were treated with cycloheximide to stop protein synthesis, followed by flow cytometry or immunoblotting to determine substrate degradation rate. Interesting mutants were then studied further with other substrates and assays.

L74A, E78A, and W123A Hrd1p Are Defective Specifically for ERAD-M

One group of mutants showed a clear specificity for integral membrane, or ERAD-M, substrates. Hrd1p variants L74A Hrd1p, E78A Hrd1p, and W123A Hrd1p were all impaired in the degradation of Hmg2p-GFP (Figure 2A). The degradation phenotypes of these mutants were not strong like a *hrd1*Δ null, which causes complete stabilization of Hmg2p-GFP (Bays et al., 2001a). Instead, the steady-state levels of the substrate were elevated, with the normalized degradation rates being similar to wild-type. This behavior of hypomorphic HRD pathway mutants can be observed in other cases, for instance in *ubx2*Δ or *usa1*Δ (Neuber et al., 2005; Schuberth and Buchberger, 2005; Figures S5B and S5C). Although there is still degradation, the efficiency of the pathway appears to be lowered so that a higher steady-state pool is required for the same degradation rate. We next examined the degradation of two other ERAD-M substrates, 6myc-Hmg2p-GFP and Pdr5*. 6myc-Hmg2p-GFP is a misfolded version of Hmg2p that does not respond to the degradation signals of the sterol pathway and, thus, is constitutively degraded (Hampton et al., 1996). All three Hrd1p mutants also stabilized 6myc-Hmg2p-GFP and Pdr5* to varying degrees (Figures 2B and 2C), with a particularly strong effect on 6myc-Hmg2p. However, their deficiencies were limited to only integral membrane proteins. We examined the degradation of both the prototype substrate CPY* and KWW and found that each ERAD-M deficient mutant was fully competent for degradation of ERAD-L substrates (Figures 2D and 2E), with no change in steady-state level or degradation rate. In all cases, the levels of

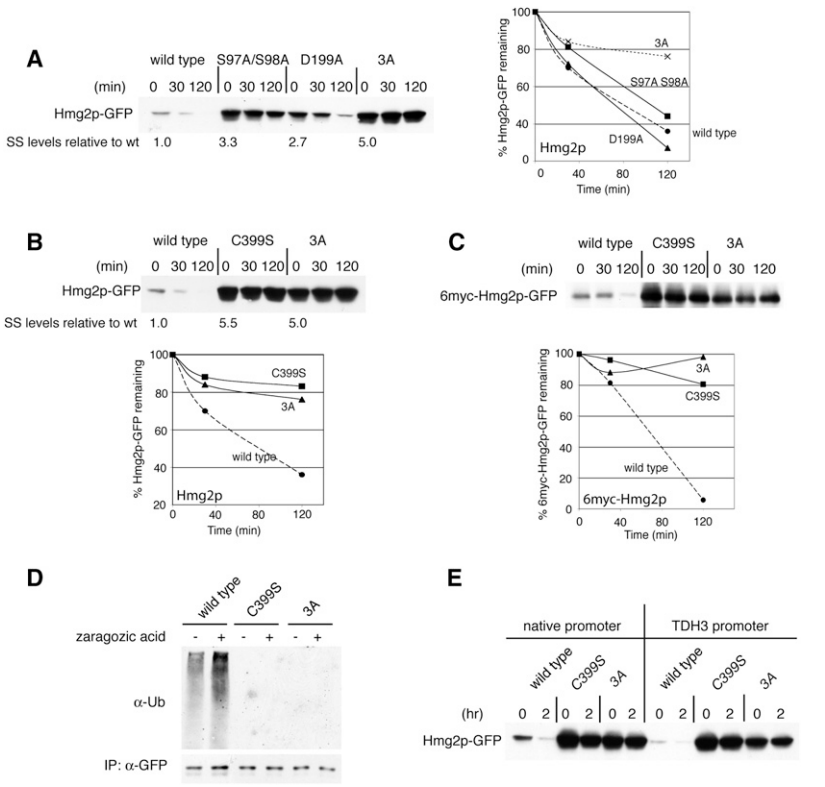

Figure 3. 3A-Hrd1p Was Incapable of Degrading or Ubiquitinating Hmg2p

(A–C) Cycloheximide chases were performed as in Figure 2. 3A-Hrd1p refers to S97A S98A D199A Hrd1p.

(D) Hmg2p-GFP ubiquitination was assayed by immunoprecipitation (IP) and ubiquitin immunoblotting. Strains were grown to log phase and treated with DMSO or 10 μg/ml zaragozic acid. Cells were lysed and subjected to an anti-GFP IP.

(E) Cycloheximide was added to *hrd1*Δ strains transformed with native promoter driven or TDH3-driven versions of *HRD1*.

each Hrd1p variant was identical to wild-type, and each underwent normal, rapid degradation in the absence of Hrd3p (data not shown). Thus, the residues mutated in L74A Hrd1p, E78A Hrd1p, and W123A Hrd1p were required for optimal ERAD-M, yet were dispensable for the degradation of misfolded lumenal substrates and Hrd1p self-degradation.

3A-Hrd1p Is Specifically Defective for Hmg2p Degradation

The above mutants showed a selective deficiency for membrane-associated substrates, without any effect on lumenal ones. This implied that ERAD-M selectivity might be determined by distinct information in the Hrd1p protein. In the next set of mutants, the specificity was even more striking, revealing distinct Hrd1p transmembrane determinants for recognition of different ERAD-M substrates. Two primary Hrd1p mutants, S97A/S98A and D199A, were partially defective in Hmg2p-GFP degradation (Figure 3A). When combined, the resulting triple mutant, S97A S98A D199A Hrd1p (3A-Hrd1p) showed a strong Hmg2p-GFP degradation block (Figure 3B), nearly identical to that of the nonfunctional C399S. 3A-Hrd1p showed a similarly strong defect in degradation of the related substrate 6myc-Hmg2p-GFP (Figure 3C).

Hrd1p is also in complex with components that mediate retrotranslocation (Carvalho et al., 2006; Denic et al., 2006). To evaluate where in the ERAD pathway 3A-Hrd1p-mediated stabilization of Hmg2p occurred, we directly tested 3A-Hrd1p for Hmg2p-GFP ubiquitination (Bays et al., 2001a). Hmg2p-GFP was ubiquitinated by wild-type Hrd1p, but not C399S Hrd1p or 3A-Hrd1p (Figure 3D). This defect was not alleviated by addition of zaragozic acid, which increases the physiological signal for Hmg2p degradation (Hampton and Bhakta, 1997).

Alteration of these three specific amino acids may have produced a hypomorphic Hrd1p mutant. To test whether higher protein expression could complement the Hmg2p degradation deficiency, we overexpressed 3A-Hrd1p by placing it behind the strong TDH3 promoter. This resulted in an approximately 20-fold increase in Hrd1p levels above the native promoter (data not shown). Nevertheless, Hmg2p-GFP degradation by overexpressed 3A-Hrd1p was still greatly impaired (Figure 3E) compared to degradation by wild-type Hrd1p. Thus, 3A-Hrd1p seemed to be intrinsically defective in Hmg2p degradation, even at high levels of this variant.

We examined the degradation of a number of ERAD-L proteins by 3A-Hrd1p. In striking contrast to Hmg2p, the degradation of the ERAD-L substrates CPY*, KHN, and KWW were all degraded normally by 3A-Hrd1p, while showing the expected stabilization in *hrd1Δ* strains (Figures 4A, 4B, and 4C). Thus, 3A-Hrd1p was completely competent for the degradation of lumenal ERAD substrates despite its near-null phenotype with Hmg2p degradation.

We tested 3A-Hrd1p with the ERAD-M substrates Pdr5* and Sec61-2p, anticipating that they would show a similarly strong block in degradation, like the weaker ERAD-M-specific mutants (see above, Figure 2). Surprisingly, Pdr5* was degraded identically by wild-type or 3A-Hrd1p (Figure 4D), but showed the expected stabilization by C399S Hrd1p. Sec61p is an essential ER protein that mediates protein translocation. Strains with the *sec61-2* mutation are temperature sensitive due to Hrd1p-mediated degradation of Sec61-2p (Biederer et al., 1996). When Hrd1p is nonfunctional, *sec61-2* strains will grow at the normally nonpermissive temperature 37°C, so a commonly utilized assay of Sec61-2p degradation is growth of *sec61-2* strains at the nonpermissive temperature (Biederer et al., 1996; Flury et al., 2005). *sec61-2* strains expressing either wild-type Hrd1p, C399S Hrd1p, or 3A-Hrd1p were grown at 30°C and 37°C. All strains grew at similar rates at 30°C. *sec61-2* strains with wild-type or 3A-Hrd1p were severely impaired for growth at elevated temperatures (Figure 4E), while those with the nonfunctional C399S Hrd1p showed robust growth at elevated temperatures

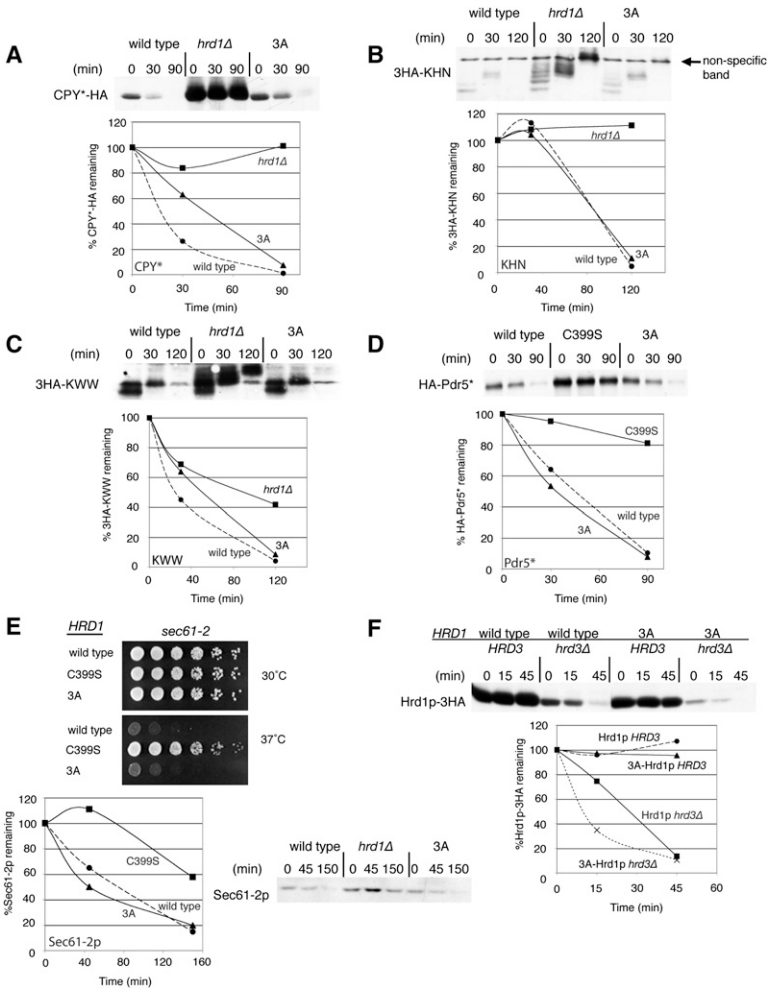

Figure 4. 3A-Hrd1p Was Proficient in the Degradation of All Other ERAD Substrates Tested

(A–D) Cycloheximide chases were performed as in Figure 2.

(E) Degradation of Sec61-2p was assayed through cycloheximide chase or growth assay. For the cycloheximide chase, strains were preincubated at 37°C for 15 min prior to drug addition. For the growth assay, strains were grown to log phase and spotted at 5-fold dilutions. Plates were grown at 30°C or 37°C for 3 days.

(F) Hrd1p self-degradation was tested by cycloheximide chase as described.

(Bordallo et al., 1998). This phenotype was confirmed through biochemical analysis of Sec61-2p stability upon cycloheximide addition. Both wild-type Hrd1p and 3A-Hrd1p were capable of Sec61-2p degradation (Figure 4E). Finally, 3A-Hrd1p stability was tested both in the presence and absence of Hrd3p by cycloheximide chase. Like wild-type Hrd1p, 3A-Hrd1p was stable in the presence of Hrd3p and underwent rapid degradation in a *hrd3Δ* strain (Figure 4F) that was RING dependent (Figure S1). Taken together, these data show that 3A-Hrd1p was impaired only in the degradation of Hmg2p-GFP (Figure 3B) or Hmg2p variants like 6myc-Hmg2p-GFP (Figure 3C), but efficiently degraded other ERAD-M and ERAD-L substrates and itself.

To get a broader sense of the degree to which 3A-Hrd1p functions normally, we evaluated the unfolded protein response (UPR) in strains harboring the 3A mutant. Loss of Hrd1p results in increased signaling through the UPR pathway (Friedlander et al., 2000). Using a GFP reporter for UPR (Bays et al., 2001b), we found that strains with the 3A-Hrd1p mutant had wild-type levels of UPR activity, while the C399S mutant strain had the expected increase in this signaling pathway (Figure S2). Thus, by this measure also, the 3A mutant showed normal function in an assay that requires recognition of what is presumably a wide variety of misfolded proteins that are typically generated during the course of normal ER function.

Distinct Hrd1p Mutants Specifically Defective for Pdr5* or Sec61-2p Degradation

3A-Hrd1p has alterations in three hydrophilic amino acids that make it incapable of recognizing Hmg2p as a misfolded protein while maintaining essentially wild-type degradation of itself and all other ERAD substrates tested. One interpretation of this observation is that distinct residues in the Hrd1p transmembrane domain mediate recognition of a given ERAD-M substrate, presumably through interactions with features of the protein that hallmark misfolding or aberrant assembly. If that was the case, we speculated that other Hrd1p transmembrane mutants in our collection that degrade Hmg2p normally would have deficiencies in degradation of a distinct ERAD-M substrate due to loss of residues needed for specific recognition of that protein. Accordingly, we rescreened our collection of Hrd1p mutants for the inability to degrade the ERAD-M substrate Pdr5*. We found two such candidates. Strains expressing only R128A Hrd1p were impaired for Pdr5* degradation (Figure 5A; Figure S3A), yet were fully proficient for Hmg2p-GFP degradation (Figure 5B; Figure S3B). Similarly, L209A showed a strong bias toward Pdr5* with a defect that rivaled C399S (Figure 5C; Figure S3C). In contrast, degradation of Hmg2p-GFP was slightly compromised, showing a small increase in steady-state levels but a wild-type degradation rate when quantified by flow cytometry (Figure 5D; Figure S3D). Sec61-2p degradation by L209A was also similar to wild-type Hrd1p as measured by the growth phenotype of the *sec61-2* strain and cycloheximide chase (Figure 5E; Figure S3E). CPY* degradation and Hrd1p self-degradation were also only slightly impaired in the L209A mutant (Figures S3F and S3G). Thus, the L209A mutant has a specific lesion that is orthogonal to that of the 3A-Hrd1p mutant: Pdr5* is stabilized to the same extent as the C399S RING mutant, while Hmg2p or Sec61-2p degradation was only very slightly affected.

The notion that the Hrd1p transmembrane domain mediates the recognition of ERAD-M substrates was further strengthened by a third mutant with a strong bias toward the final test substrate, Sec61-2p. Upon screening the collection of variants,

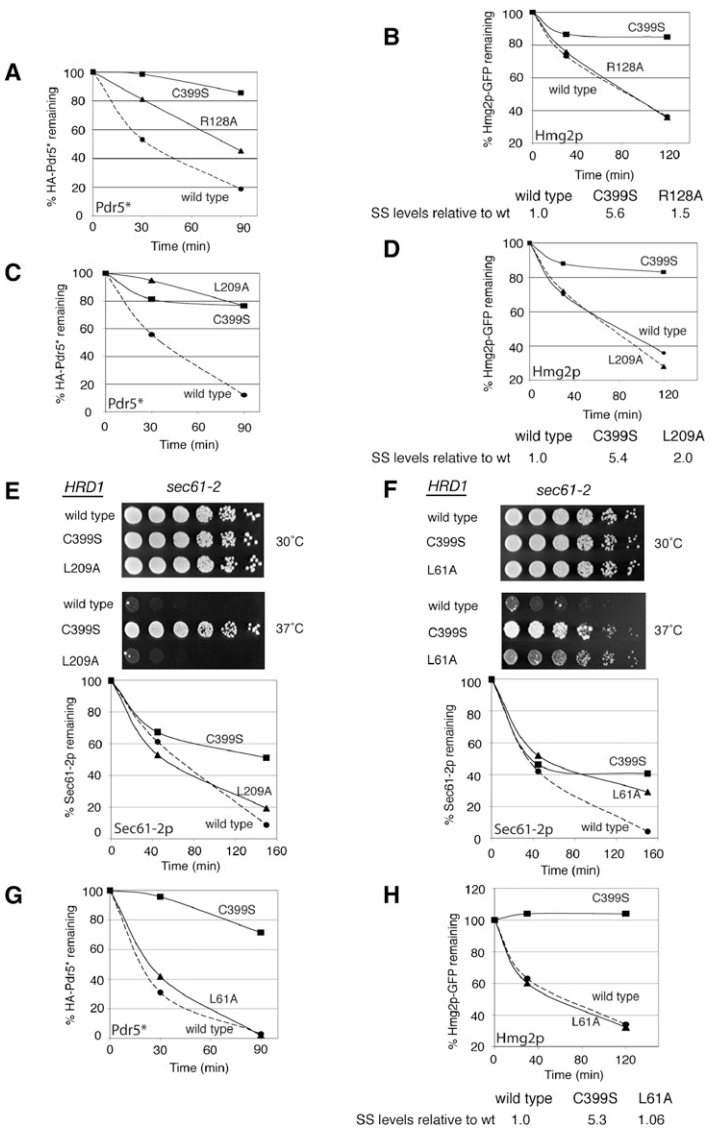

Figure 5. Distinct Hrd1p Mutants Were Specifically Deficient for Pdr5* or Sec61-2p Degradation

(A–D) Cycloheximide chases were performed as in Figure 2.

(E and F) Sec61-2p stability was measured by cycloheximide chase and growth assay at 30°C or 37°C as in Figure 4.

(G and H) Cycloheximide chases were performed as previously described. Western blots for all biochemical results in Figure 5 can be found in the Figures S3 and S4.

a single point mutant, L61A, was found that partially stabilized only this substrate as measured through both growth of *sec61-2* strains at the nonpermissive temperature and biochemical analysis (Figure 5F; Figure S4A). There was no effect of this mutant on Pdr5* or Hmg2p-GFP degradation (Figures 5G and 5H; Figure S4B). To verify that the Sec61-2p phenotype was not due to a temperature-specific defect of L61A Hrd1p, we examined L61A Hrd1p stability, Hmg2p-GFP degradation, and Pdr5* degradation at 37°C. In all cases, L61A Hrd1p behaved like wild-type Hrd1p (Figures S4C, S4D, and S4E). Taken together, the unique substrate specificities of 3A-Hrd1p, L209A Hrd1p, and L61A Hrd1p indicate that the Hrd1p transmembrane domain mediates recognition of ERAD-M substrates.

The 3A-Hrd1p Phenotype Is Not Dependent on Other ERAD Factors

The above experiments indicate that ERAD-M substrate specificity requires information in the Hrd1p transmembrane domain. We focused our attention on the 3A-Hrd1p mutant to further understand the mechanism of ERAD-M substrate recognition mediated by the Hrd1p transmembrane domain.

In studies concerning the recognition of misfolded ER proteins, a number of ERAD complex members have been implicated in the degradation of lumenal substrates. These include Yos9p, Der1p, Hrd3p, Usa1p, and Ubx2p (Carvalho et al., 2006; Denic et al., 2006). In contrast, Hrd1p-dependent degradation of membrane proteins can proceed, often at wild-type rates, in the absence of these proteins. For example, Hmg2p degradation proceeds normally in a *yos9Δ* null (Figure 6A) and in the *hrd3Δ* null if levels of Hrd1p are sufficiently elevated to overcome its rapid degradation (Gardner et al., 2000). As a test of the autonomy of Hmg2p recognition mediated by the mutated 3A-Hrd1p residues, we compared the 3A mutant to wild-type Hrd1p in a number of ERAD component null strains, using cycloheximide chases as above. The nulls included *yos9Δ*, *usa1Δ*, *ubx2Δ*, *der1Δ*, and *hrd3Δ*. In all cases, the strong stabilizing phenotype of 3A-Hrd1p was unaffected, while Hmg2p-GFP degradation occurred in wild-type Hrd1p-expressing strains. The normalized data are presented in Figures 6A–6D and the western blots are shown in Figures S5A–S5D. In the *usa1Δ* and *ubx2Δ* strains, a mild hypomorphic HRD phenotype was observed as elevated Hmg2p-GFP steady-state levels in the blots (Figures S5B and S5C). Nevertheless, the 3A-Hrd1p mutant had strong effects on degradation in all cases. In the *hrd3Δ* null, we overexpressed Hrd1p to overcome the drastic loss of the protein that occurs in the absence of Hrd3p and used flow cytometry to analyze the effects on the Hmg2p-GFP substrate (Figure 6E). In all cases, the striking difference between Hrd1p and 3A-Hrd1p in Hmg2p-GFP degradation was evident and not dependent on any of the HRD components tested.

The Hrd1p ligase is in complex with a number of proteins including the factors tested as nulls above (Carvalho et al., 2006; Denic et al., 2006). The ability of 3A-Hrd1p to efficiently degrade all non-Hmg2p substrates implied that the HRD complex was intact. We directly examined documented interactions between Hrd1p and a number of HRD complex members. Using a native coimmunoprecipitation (co-IP) derived from the previous studies of the HRD complex (Gardner et al., 2000), we tested the interactions of 3HA-tagged native or 3A-Hrd1p with Yos9p-Flag, Hrd3p-3HA, Ubx2p-3HA, Usa1p-6HA, and Protein A-Cdc48p (Denic et al., 2006; Gardner et al., 2000; Sato and Hampton, 2006; Schuberth and Buchberger, 2005). Lysates of strains coexpressing each tagged pair were prepared, and then microsomes were isolated and immunoprecipitated with

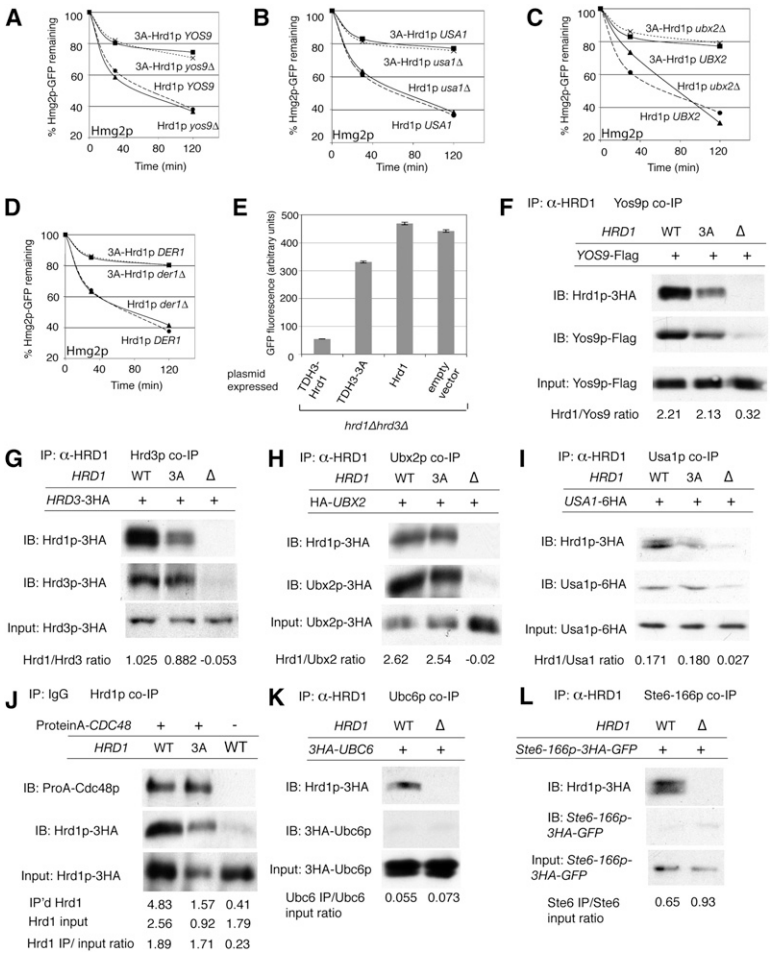

Figure 6. The Role of Other ERAD Factors in Hmg2p-GFP Degradation Is Unaltered by 3A-Hrd1p

(A–E) Hmg2p-GFP degradation was assayed in isogenic wild-type and the indicated null strains expressing either wild-type or 3A-Hrd1p as in Figure 2.

(F–I) The association between wild-type or 3A-Hrd1p was tested with other ERAD factors by co-IP. Microsomes were isolated and subjected to an anti-HRD1 IP. Due to the differences in levels between wild-type and 3A-Hrd1p, the ratio of Hrd1p immunoprecipitated was compared to the indicated protein.

(J) The association between wild-type or 3A-Hrd1p with Protein A-Cdc48p was tested in a co-IP. Protein A-Cdc48 was immunoprecipitated with IgG-Sepharose beads.

(K and L) The association between wild-type or 3A-Hrd1p was tested with Ubc6p and Ste6-166p in a co-IP as described.

polyclonal anti-Hrd1p antibodies, or in the case of Cdc48p, IgG-Sepharose beads. This was followed by SDS-PAGE and immunoblotting for the Hrd1p or test proteins indicated (Figures 6F–6J). For each experiment, a strain containing an empty vector (instead of a Hrd1p-expressing plasmid) was included as a control. The intensity of each band was measured by a Typhoon 9400 and ImageQuant 5.2 software, and the values for these measurements are depicted. The interaction of Hrd1p and 3A-Hrd1p with the ERAD factors tested was similar when the slightly lower steady-state levels of 3A-Hrd1p were normalized for, by calculating the ratio of Hrd1p and the indicated ERAD component. As negative controls, we tested the binding of Hrd1p to two ER membrane proteins that are neither HRD complex members nor HRD substrates. These were the E2, 3HA-Ubc6p and Ste6-166p-3HA-GFP, which are both Doa10p substrates (Huyer et al., 2004; Swanson et al., 2001). Neither interacted with Hrd1p (Figures 6K and 6L), demonstrating that the association between wild-type or 3A-Hrd1p and the Hrd1p-associated complex members was specific.

In Vitro Studies of 3A-Hrd1p

We next turned our attention to the role the residues defined by the 3A mutation played in Hmg2p recognition. Clearly, E3 ligases must bind a targeted substrate to transfer ubiquitin. However, it is not generally known if substrates need only to bind to ligases, or if in addition, the substrate must activate or transmit information to the ligase to bring about robust polyubiquitination. Our crosslinking studies indicate that for Hrd1p, the latter model might be the case (Gardner et al., 2001b). Hrd1p crosslinks degraded substrates Hmg2p and 6myc-Hmg2p, but also nondegraded K6R-Hmg2p or the highly stable homolog Hmg1p with similar efficiencies (Gardner et al., 2001b). Likewise, improving the folding of Hmg2p with the chemical chaperone glycerol prohibits Hrd1p-dependent ubiquitination (R. Garza and R.Y.H., unpublished data), but not Hmg2p-Hrd1p crosslinking (Gardner et al., 2001b). Thus, substrate interaction by this criterion appears to be insufficient for Hrd1p-mediated ubiquitination.

We tested whether Hmg2p-GFP was capable of interacting with 3A-Hrd1p by two approaches. We first utilized an in vitro crosslinking assay, in which ER-enriched microsomes were harvested from cells expressing Hmg2p-GFP with wild-type or 3A-Hrd1p tagged with triple HA. The lipid-soluble crosslinker DSP was added to the microsomes, followed by an anti-GFP immunoprecipitation. The precipitated protein mixture was then immunoblotted for Hmg2p-GFP or Hrd1p-3HA after SDS-PAGE. Both wild-type and 3A-Hrd1p associated with Hmg2p-GFP in a crosslinker-dependent manner (Figure 7A).

We also evaluated the Hmg2p-Hrd1p interaction with a nondenaturing co-IP assay. Microsomes were isolated and added to a 1.5% Tween-20 lysis buffer. An anti-GFP antibody was then added to the lysates in order to immunoprecipitate Hmg2p-GFP, and coprecipitated Hrd1p was then detected with anti-HA immunoblotting. Under these conditions, Hmg2p-GFP bound to wild-type or 3A-Hrd1p with equal efficiency (Figure 7B). This interaction was specific, as a control immunoprecipitation with a strain lacking Hmg2p-GFP was unable to pull down Hrd1p. Conversely, two integral membrane proteins (Ubc6p and Ste6-166p) that are substrates of the Doa10 ERAD pathway failed to coprecipitate with Hrd1p (Figures 6K and 6L). Thus, 3A-Hrd1p was capable of binding to Hmg2p-GFP. Identical results were observed in both *UBC7* (data not shown) and *ubc7Δ* strains

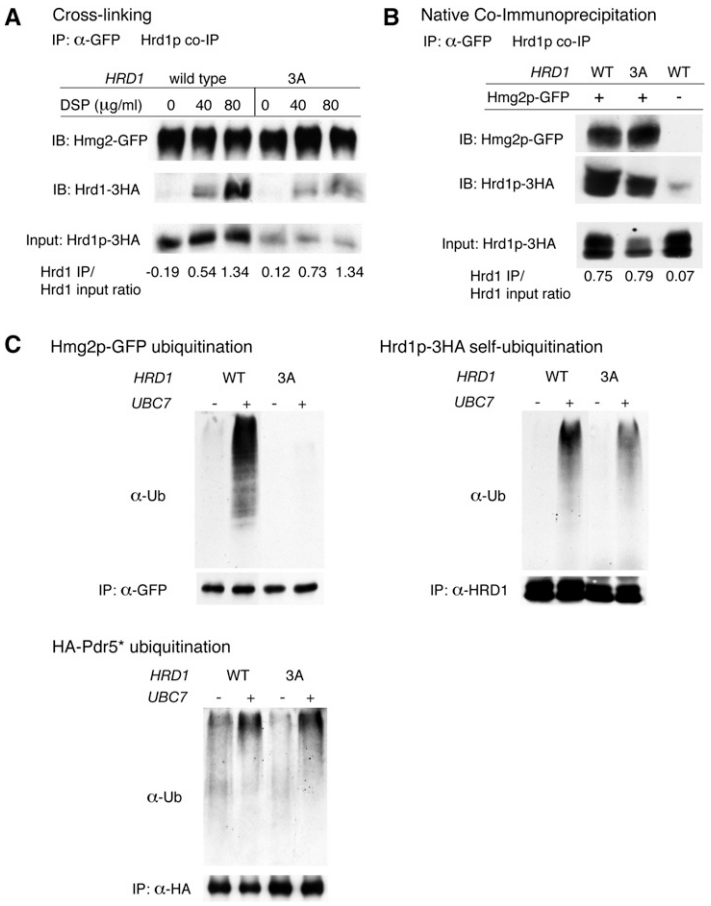

Figure 7. In Vitro Analysis of 3A-Hrd1p Interaction and Ubiquitination of Hmg2p-GFP

(A) Isogenic strains expressing wild-type or 3A-Hrd1p tagged with 3HA and Hmg2p-GFP were grown to log phase. Microsomes were harvested and DMSO or increasing concentrations of the crosslinker DSP were added. An anti-GFP IP was then performed, and Hmg2p-GFP and Hrd1p-3A levels were measured by SDS-PAGE and immunoblotting (IB) as described in methods.

(B) A native co-IP was performed with *ubc7*Δ microsomes isolated from strains with or without Hmg2p-GFP and expressing 3HA-tagged wild-type or 3A-Hrd1p.

(C) The same microsomes utilized in (B) were added to cytosol from strains overexpressing Ubc7p-2HA to assay in vitro ubiquitination of the indicated protein. Microsomes, cytosol, and ATP were incubated for 1 hr at 30°C and then subjected to an IP. The observed ubiquitination was absent when microsomes were incubated with *ubc7*Δ cytosol.

(Figure 7B). The *ubc7Δ* strains were necessary in order to test for in vitro substrate ubiquitination as described next.

We used the same microsomes prepared for the native co-IP experiment to directly evaluate the ability of the 3A-Hrd1p to ubiquitinate Hmg2p-GFP in an in vitro ubiquitination assay. In this assay, microsome strains lacking Ubc7p and cytosol strains with or without Ubc7p, but lacking Hrd1p and Hmg2p-GFP, were utilized as described (Flury et al., 2005 and Experimental Procedures). Microsomes, cytosol, and ATP were incubated for 1 hr at 30°C, allowing substrate ubiquitination followed by IP and immunoblotting for ubiquitin and Hmg2p-GFP. Wild-type Hrd1p ubiquitinated Hmg2p-GFP in vitro while 3A-Hrd1p did not (Figure 7C). This defect was specific for Hmg2p, as 3A-Hrd1p demonstrated self-ubiquitination in the same in vitro reaction and was also capable of transferring ubiquitin to Pdr5* (Figure 7C). In vitro ubiquitination was Hrd1p, Ubc7p, and Hrd1p RING dependent (Figure S6; Figure 7C). Although Hrd1p and Hmg2p-GFP binding was unaffected by the introduction of the 3A mutations, 3A-Hrd1p could not ubiquitinate Hmg2p-GFP, indicating that substrate binding alone is insufficient to trigger Hrd1p-dependent ubiquitination.

DISCUSSION

The recognition of misfolded proteins is a central and unresolved process in all protein quality-control pathways. The diversity of substrates indicates that structural features serve as criteria for substrate recognition. Since E3 ligases are critical definers of specificity, misfolded substrate detection must include, in some manner, the ligase.

For Hrd1p, both lumenal (ERAD-L) and integral membrane (ERAD-M) substrates are targets for degradation. Recognition of ERAD-L substrates relies heavily on Hrd1p-associated factors such as Yos9p, Kar2p, and the lumenal domain of Hrd3p (Carvalho et al., 2006; Denic et al., 2006).

In contrast, Hrd1p appears to mediate the recognition of integral membrane substrates, as is demonstrated by the discovery of mutants highly selective for individual ERAD-M substrates. Thus, extreme specificity for ERAD-M substrate recognition lies in the transmembrane domain of Hrd1p. This ability of the Hrd1p transmembrane domain to discern substrates was an autonomous feature of the protein: the high selectivity of the residues altered in the 3A mutant was not dependent on any ERAD factors tested.

Interestingly, none of our mutants had selective defects in ERAD-L. This implies that distinct rules govern recognition of ERAD-M substrates, although a more complete analysis of Hrd1p is needed to fully test the idea that ERAD-L recognition lies outside of the membrane anchor. It is worth noting that the ERAD-C pathway responsible for degrading proteins with misfolded cytosolic domains requires cytosolic chaperones for Doa10p-dependent ubiquitination (Nakatsukasa et al., 2008). Thus, the lack of involvement of such factors and the autonomous requirement for the Hrd1p membrane domain indicates that ERAD-M employs recognition rules distinct from those used for soluble determinants of misfolding.

An Allosteric Model for Hrd1p-Dependent Ubiquitination

3A-Hrd1p is essentially a phenocopy of a C399S RING mutant, but only for Hmg2p-related substrates. Both crosslinking and co-IP assay showed that the 3A-Hrd1p-Hmg2p interaction was intact. Importantly, Hrd1p was unable to co-precipitate two integral membrane DOA-pathway substrates. Thus, although the co-IP assay showed the appropriate specificity for Hmg2p-GFP, it was not affected in the strong 3A mutant. However, in vitro 3A-Hrd1p did not support ubiquitination of Hmg2p, yet

still functioned in vitro as a ligase, showing normal self and Pdr5* ubiquitination. Thus, the high specificity of the 3A mutation is not due to any measurable loss of interaction with Hmg2p but, rather, to an inability of the still-active 3A-Hrd1p mutant to transfer ubiquitin to Hmg2p that is in its proximity.

In our earlier interaction studies, we had noted that Hrd1p was able to associate with potential substrates in a fairly indiscriminant manner. We proposed that Hrd1p queries a variety of proteins by low-specificity interactions, and only when a given substrate has the appropriate structural features does ubiquitination occur. Likewise, while 3A-Hrd1p binds to Hmg2p, it appears to be incapable of transmitting the structural information to the RING domain to promote ubiquitination, thus supporting an ''allosteric'' model for Hrd1p selectivity in which the specificity of substrate ubiquitination lies downstream of low-affinity ligase-substrate interactions (Figure S7).

Alternatively, it may be that the residues altered in the 3A mutant do indeed inhibit a high-affinity interaction with Hmg2p not detected by our assays, although the same techniques have been used successfully to detect substrate-E3 interactions that do determine selectivity (Denic et al., 2006; Schuberth and Buchberger, 2005). However, we favor the model of structural evaluation determined subsequent to low-specificity engagement of substrate with the HRD complex. At least for quality control substrates, this strategy of ''general interaction-specific response'' makes some teleological sense. A quality control ligase that is over-dedicated to interacting with only a particular type of substrate would not be efficient in the general detection of the very large number of possible misfolded proteins that it might encounter.

Separable Determinants of Substrate Recognition by Hrd1p

The detection of ERAD-M substrates, that is, misfolded or unassembled membrane proteins, might be expected to follow rules distinct from those used to detect ERAD-L substrates. A misfolded aqueous protein would display a larger-than-normal proportion of surface hydrophobic residues, and indeed, proteins that detect misfolded soluble proteins, such as chaperones or UGGT (Dejgaard et al., 2004), have regions that can interact with exposed hydrophobic regions of their clients. Conversely, misfolded integral membrane proteins perhaps expose normally buried hydrophilic residues to the lipid region of the bilayer. Detection of these inappropriate residues could be accomplished by interaction with membrane-embedded hydrophilic residues on the ligase. Consistent with this, the 3A mutant of Hrd1p has three intramembrane residues changed from S, S and D to alanine. Extensive Hmg2p structural analysis has also uncovered conserved hydrophilic residues within the transmembrane spans that, when mutated, result in a completely stable protein (T. Davis and R.Y.H., unpublished data). Similarly, it has been suggested that the TUL1 ubiquitin ligase recognizes unassembled membrane protein clients through interactions between hydrophilic intramembrane residues (Reggiori and Pelham, 2002). It is interesting to note that the quality control ligases mammalian Hrd1, gp78, and yeast Doa10p each have a high density of intramembrane hydrophilic residues, as would be expected if hydrophilic scanning was a general strategy for membrane substrate evaluation. These examples indicate that recognition of hydrophilic intramembrane residues on a misfolded protein by similar residues within a ligase may be a broadly employed strategy.

Direct loss of such ''hydrophilic scanning'' residues is probably not the only lesion in some of our mutants. L209A Hrd1p, which has slight general ERAD defects but is completely incapable of Pdr5* degradation, has a missing intramembrane leucine, and presumably this alteration creates a structural change that specifically alters Pdr5* binding or evaluation. Similarly the Sec61-2-selective L61A Hrd1p mutant has an intramembrane hydrophobic residue replaced by alanine. It may be that the changes of hydrophobic residues alter the position of key hydrophilic residues or that other structural features that assist in substrate detection are being altered. With regard to the question of the functions of these residues, it will be most revealing when the structure of the Hrd1p transmembrane domain is solved by high resolution techniques in the future.

Taken together, these studies imply that the Hrd1p transmembrane domain specifically mediates ERAD-M. It appears that the transmembrane domain bears a structural code for detection of features that hallmark a degradation substrate, and this information appears to be multifaceted, so that the loss of recognition of a single substrate class can be observed in the appropriate mutant. Eventually, unraveling this code will help us understand the rules by which misfolded proteins are led to their destruction.

EXPERIMENTAL PROCEDURES

Plasmid Construction, Yeast, and Bacterial Strains

All plasmids were constructed as described (Sato and Hampton, 2006). A detailed description and complete plasmid table is provided in the Supplemental Data.

Escherichia coli DH5α were grown in LB media with ampicillin. Yeast strains were grown at 30°C unless noted in minimal media supplemented with dextrose and amino acids (Hampton and Rine, 1994). A complete description of strain construction and a list of all parent strains, the plasmids transformed into them, and the figures in which they were utilized are listed in the Supplemental Data.

Degradation Assays and UPR Measurements

Cycloheximide chase degradation assays and flow cytometry were performed as previously described (Sato and Hampton, 2006). All non-GFP strain quantitation was performed using a Typhoon 9400 and ImageQuant 5.2 software (GE Healthcare, Piscataway, NJ). In these cases, a representative western blot was quantified and the data points were graphed.

Ubiquitination Assay

Ubiquitination of Hmg2p-GFP was examined in log phase cells as previously described (Bays et al., 2001a) by immunoprecipitation (IP) followed by ubiquitin or substrate immunoblotting. A more detailed description can be found in the Supplemental Data.

Crosslinking Assay

Crosslinking was modified from that used by Gardner et al., (2000 and 2001b) and is described in detail in the Supplemental Data. Microsomes were harvested in B88 buffer and incubated with the crosslinker DSP for 40 min at 22°C. The crosslinker was quenched in 50 mM Tris (pH 7.5), and the microsomes were centrifuged and lysed in SUME lysis buffer plus 1% Triton X-100 and 0.5% DOC. IP buffer was then added to each sample along with anti-GFP antibody. The remainder of the IP was performed as described.

Native Coimmunoprecipitation

The native co-IP assay was adapted from Gardner et al. (2000) and described in the Supplemental Data. Briefly, microsomes were harvested as in the cross-linking protocol, except it was performed in MF buffer. Pelleted microsomes were resuspended in 1 ml of Tween buffer and incubated on ice for 15 min. Lysates were then centrifuged for 30 min at 14,000 × g. The remainder of the IP was performed as described except the Tween-20 buffer was utilized for washes.

Dilution Assays

Growth of *sec61-2* strains was measure by dilution assay, performed as described (Sato and Hampton, 2006) and in the Supplemental Data.

In Vitro Ubiquitination

In vitro ubiquitination assays were performed as described (Flury et al., 2005). Briefly, *ubc7Δ* microsome strains, containing TDH3-Hrd1-3HA (wild-type or 3A) and the indicated substrate were utilized. Microsomes were prepared identically as in the native co-IP experiments and were resuspended in B88 buffer. Cytosol strains underwent freeze-thaw lysis in B88 buffer and ultracentrifuged. For each ubiquitination reaction, a microsome strain was combined with 30 mM ATP and cytosol that either did or did not contain TDH3-Ubc7-2HA for 1 hr at 30°C. The IP was then performed as described.

SUPPLEMENTAL DATA

The Supplemental Data include three tables, Supplemental Experimental Procedures, and seven figures and can be found with this article online at http://www.cell.com/molecular-cell/supplemental/S1097-2765(09)00200-7.

ACKNOWLEDGMENTS

We thank Alexander Buchberger (Max Planck Institute of Biochemistry), Davis Ng (National University of Singapore), Randy Schekman (University of California, Berkeley), Thomas Sommer (Max-Delbruck Center for Molecular Medicine), Jonathan Weissman (University of California, San Francisco), and Dieter Wolf (University of Stuttgart) for providing plasmids, strains, and antibodies; Maho Niwa (University of California, San Diego) for use of the Typhoon 9400; and Michael David (University of California, San Diego) for use of the flow microfluorimeter, despite our preference for avid yeast. We also thank the Hampton laboratory for enthusiastic and incisive discussions and technical assistance. Finally, R.Y.H. would like to thank his brothers Ron and Bob for lifelong sibling support, spiritual growth, and genetic connection. These studies were supported by NIH grant 5 R01 DK051996-15 to R.Y.H. B.K.S. was a trainee under the NIH Genetic Training grant no. 5T32GM008666.

Received: July 22, 2008
Revised: December 12, 2008
Accepted: March 20, 2009
Published: April 23, 2009

REFERENCES

Amano, T., Yamasaki, S., Yagishita, N., Tsuchimochi, K., Shin, H., Kawahara, K., Aratani, S., Fujita, H., Zhang, L., Ikeda, R., et al. (2003). Synoviolin/Hrd1, an E3 ubiquitin ligase, as a novel pathogenic factor for arthropathy. Genes Dev. *17*, 2436–2449.

Bays, N.W., Gardner, R.G., Seelig, L.P., Joazeiro, C.A., and Hampton, R.Y. (2001a). Hrd1p/Der3p is a membrane-anchored ubiquitin ligase required for ER-associated degradation. Nat. Cell Biol. *3*, 24–29.

Bays, N.W., Wilhovsky, S.K., Goradia, A., Hodgkiss-Harlow, K., and Hampton, R.Y. (2001b). HRD4/NPL4 is required for the proteasomal processing of ubiquitinated ER proteins. Mol. Biol. Cell *12*, 4114–4128.

Bazirgan, O.A., Garza, R.M., and Hampton, R.Y. (2006). Determinants of RING-E2 fidelity for Hrd1p, a membrane-anchored ubiquitin ligase. J. Biol. Chem. *281*, 38989–39001.

Biederer, T., Volkwein, C., and Sommer, T. (1996). Degradation of subunits of the Sec61p complex, an integral component of the ER membrane, by the ubiquitin-proteasome pathway. EMBO J. *15*, 2069–2076.

Bordallo, J., Plemper, R.K., Finger, A., and Wolf, D.H. (1998). Der3p/Hrd1p is required for endoplasmic reticulum-associated degradation of misfolded lumenal and integral membrane proteins. Mol. Biol. Cell *9*, 209–222.

Carvalho, P., Goder, V., and Rapoport, T.A. (2006). Distinct ubiquitin-ligase complexes define convergent pathways for the degradation of ER proteins. Cell *126*, 361–373.

Deak, P.M., and Wolf, D.H. (2001). Membrane topology and function of Der3/Hrd1p as a ubiquitin-protein ligase (E3) involved in endoplasmic reticulum degradation. J. Biol. Chem. *276*, 10663–10669.

Dejgaard, S., Nicolay, J., Taheri, M., Thomas, D.Y., and Bergeron, J.J. (2004). The ER glycoprotein quality control system. Curr. Issues Mol. Biol. *6*, 29–42.

Denic, V., Quan, E.M., and Weissman, J.S. (2006). A luminal surveillance complex that selects misfolded glycoproteins for ER-associated degradation. Cell *126*, 349–359.

Flury, I., Garza, R., Shearer, A., Rosen, J., Cronin, S., and Hampton, R.Y. (2005). INSIG: a broadly conserved transmembrane chaperone for sterol-sensing domain proteins. EMBO J. *24*, 3917–3926.

Friedlander, R., Jarosch, E., Urban, J., Volkwein, C., and Sommer, T. (2000). A regulatory link between ER-associated protein degradation and the unfolded-protein response. Nat. Cell Biol. *2*, 379–384.

Gardner, R.G., and Hampton, R.Y. (1999). A highly conserved signal controls degradation of 3-hydroxy-3-methylglutaryl-coenzyme A (HMG-CoA) reductase in eukaryotes. J. Biol. Chem. *274*, 31671–31678.

Gardner, R.G., Swarbrick, G.M., Bays, N.W., Cronin, S.R., Wilhovsky, S., Seelig, L., Kim, C., and Hampton, R.Y. (2000). Endoplasmic reticulum degradation requires lumen to cytosol signaling. Transmembrane control of Hrd1p by Hrd3p. J. Cell Biol. *151*, 69–82.

Gardner, R.G., Shan, H., Matsuda, S.P., and Hampton, R.Y. (2001a). An oxysterol-derived positive signal for 3-hydroxy- 3-methylglutaryl-CoA reductase degradation in yeast. J. Biol. Chem. *276*, 8681–8694.

Gardner, R.G., Shearer, A.G., and Hampton, R.Y. (2001b). In vivo action of the HRD ubiquitin ligase complex: mechanisms of endoplasmic reticulum quality control and sterol regulation. Mol. Cell. Biol. *21*, 4276–4291.

Goldstein, J.L., and Brown, M.S. (1990). Regulation of the mevalonate pathway. Nature *343*, 425–430.

Hampton, R.Y. (2002a). ER-associated degradation in protein quality control and cellular regulation. Curr. Opin. Cell Biol. *14*, 476–482.

Hampton, R.Y. (2002b). Proteolysis and sterol regulation. Annu. Rev. Cell Dev. Biol. *18*, 345–378.

Hampton, R.Y., and Rine, J. (1994). Regulated degradation of HMG-CoA reductase, an integral membrane protein of the endoplasmic reticulum, in yeast. J. Cell Biol. *125*, 299–312.

Hampton, R.Y., and Bhakta, H. (1997). Ubiquitin-mediated regulation of 3-hydroxy-3-methylglutaryl-CoA reductase. Proc. Natl. Acad. Sci. USA *94*, 12944–12948.

Hampton, R.Y., and Garza, R.M. (2009). Protein Quality Control as a Strategy for Cellular Regulation: Lessons from Ubiquitin-Mediated Regulation of the Sterol Pathway. Chemical Rev. Published online February 25, 2009. 10. 1021/cr800544v.

Hampton, R.Y., Gardner, R.G., and Rine, J. (1996). Role of 26S proteasome and HRD genes in the degradation of 3-hydroxy-3-methylglutaryl-CoA reductase, an integral endoplasmic reticulum membrane protein. Mol. Biol. Cell *7*, 2029–2044.

Huyer, G., Piluek, W.F., Fansler, Z., Kreft, S.G., Hochstrasser, M., Brodsky, J.L., and Michaelis, S. (2004). Distinct machinery is required in Saccharomyces cerevisiae for the endoplasmic reticulum-associated degradation of a multispanning membrane protein and a soluble luminal protein. J. Biol. Chem. *279*, 38369–38378.

Jakob, C.A., Bodmer, D., Spirig, U., Battig, P., Marcil, A., Dignard, D., Bergeron, J.J., Thomas, D.Y., and Aebi, M. (2001). Htm1p, a mannosidase-like protein, is involved in glycoprotein degradation in yeast. EMBO Rep. *2*, 423–430.

Knop, M., Finger, A., Braun, T., Hellmuth, K., and Wolf, D.H. (1996). Der1, a novel protein specifically required for endoplasmic reticulum degradation in yeast. EMBO J. *15*, 753–763.

Liang, J., Yin, C., Doong, H., Fang, S., Peterhoff, C., Nixon, R.A., and Monteiro, M.J. (2006). Characterization of erasin (UBXD2): a new ER protein that promotes ER-associated protein degradation. J. Cell Sci. *119*, 4011–4024.

Nakatsukasa, K., Huyer, G., Michaelis, S., and Brodsky, J.L. (2008). Dissecting the ER-associated degradation of a misfolded polytopic membrane protein. Cell *132*, 101–112.

Neuber, O., Jarosch, E., Volkwein, C., Walter, J., and Sommer, T. (2005). Ubx2 links the Cdc48 complex to ER-associated protein degradation. Nat. Cell Biol. *7*, 993–998.

Plemper, R.K., Egner, R., Kuchler, K., and Wolf, D.H. (1998). Endoplasmic reticulum degradation of a mutated ATP-binding cassette transporter Pdr5 proceeds in a concerted action of Sec61 and the proteasome. J. Biol. Chem. *273*, 32848–32856.

Ravid, T., Kreft, S.G., and Hochstrasser, M. (2006). Membrane and soluble substrates of the Doa10 ubiquitin ligase are degraded by distinct pathways. EMBO J. *25*, 533–543.

Reggiori, F., and Pelham, H.R. (2002). A transmembrane ubiquitin ligase required to sort membrane proteins into multivesicular bodies. Nat. Cell Biol. *4*, 117–123.

Richly, H., Rape, M., Braun, S., Rumpf, S., Hoege, C., and Jentsch, S. (2005). A series of ubiquitin binding factors connects CDC48/p97 to substrate multiubiquitylation and proteasomal targeting. Cell *120*, 73–84.

Sato, B.K., and Hampton, R.Y. (2006). Yeast Derlin Dfm1 interacts with Cdc48 and functions in ER homeostasis. Yeast *23*, 1053–1064.

Schuberth, C., and Buchberger, A. (2005). Membrane-bound Ubx2 recruits Cdc48 to ubiquitin ligases and their substrates to ensure efficient ER-associated protein degradation. Nat. Cell Biol. *7*, 999–1006.

Swanson, R., Locher, M., and Hochstrasser, M. (2001). A conserved ubiquitin ligase of the nuclear envelope/endoplasmic reticulum that functions in both ER-associated and Matalpha2 repressor degradation. Genes Dev. *15*, 2660–2674.

Vashist, S., and Ng, D.T. (2004). Misfolded proteins are sorted by a sequential checkpoint mechanism of ER quality control. J. Cell Biol. *165*, 41–52.

Voges, D., Zwickl, P., and Baumeister, W. (1999). The 26S proteasome: a molecular machine designed for controlled proteolysis. Annu. Rev. Biochem. *68*, 1015–1068.

Zhang, Y., Michaelis, S., and Brodsky, J.L. (2002). CFTR expression and ER-associated degradation in yeast. Methods Mol. Med. *70*, 257–265.

Molecular Cell, Volume *34*

Supplemental Data

Misfolded Membrane Proteins Are Specifically Recognized by the Transmembrane Domain of the Hrd1p Ubiquitin Ligase

Brian K. Sato, Daniel Schulz, Phong H. Do, and Randolph Y. Hampton

Table S1. Plasmids used in this study

Plasmid	Gene expressed
pRH311	*YIp TRP1*
pRH313	*YIp URA3*
pRH469	*YIp URA3 pTDH3-HMG2-GFP*
pRH507	*YIp TRP1 pHRD1*
pRH642	*YIp TRP1 pHRD1-3HA*
pRH730	*YIp TRP1 pTDH3-HRD1-3HA*
pRH808	*YIp TRP1 pTDH3-HRD1*
pRH1122	*hrd1Δ::KanMX deletion cassette*
pRH1151	*YIp URA3 pTDH3-3HA-UBC6*
pRH1152	*YIp LEU2 pTDH3-UBC7-2HA*
pRH1209	*YIp URA3 p4XUPRE-GFP*
pRH1245	*YIp TRP1 pHRD1-3HA C399S*
pRH1301	*YIp ADE2 pHRD3-3HA*
pRH1377	*YCp URA3 pCPY*-HA*
pRH1694	*YIp URA3 pTDH3-6MYC-HMG2-GFP*
pRH1718	*YIp TRP1 pTDH3-HRD1-3HA C399S*
pRH1958	*Ycp URA3 p3HA-KHN*
pRH1960	*Ycp URA3 p3HA-KWW*
pRH2058	*2μ URA3 pPGK-STE6-166-3HA-GFP*

pRH2078	*YCp LEU2 pNOPPA-PROTEIN A-CDC48*
pRH2115	*2μ LEU2 YOS9-FLAG*
pRH2213	*YIp TRP1 pHRD1-3HA S97A S98A*
pRH2248	*YIp TRP1 pHRD1-3HA D199A*
pRH2269	*YIp TRP1 pHRD1-3HA S97A S98A D199A*
pRH2287	*YIp TRP1 pHRD1-3HA S97A S98A D199A C399S*
pRH2288	*YIp TRP1 pHRD1 S97A S98A D199A*
pRH2312	*YCp HIS3 pHA-PDR5**
pRH2316	*YIp TRP1 pHRD1-3HA L61A*
pRH2344	*YIp TRP1 pHRD1-3HA L74A*
pRH2345	*YIp TRP1 pHRD1-3HA E78A*
pRH2350	*YIp TRP1 pHRD1-3HA W123A*
pRH2352	*YIp TRP1 pHRD1-3HA R128A*
pRH2360	*YIp TRP1 pHRD1-3HA L209A*
pRH2361	*YIp TRP1 pHRD1 L74A*
pRH2362	*YIp TRP1 pHRD1 E78A*
pRH2364	*YIp TRP1 pHRD1 W123A*
pRH2365	*YIp TRP1 pTDH3-HRD1-3HA S97A S98A D199A*
pRH2366	*YIp TRP1 pTDH3-HRD1 S97A S98A D199A*
pRH2398	*YIp TRP1 pHRD1 L209A*
pRH2517	*YIp TRP1 pTDH3-HRD1-3HA S97A S98A D199A C399S*

Table S2. Strains used in this study

Strain	Genotype
RHY2814	*MATα ade2-101 ura3-52::URA3::HMGcd::HMG2-GFP met2 lys2-801 trp1::hisG leu2Δ his3Δ200 hmg1Δ::LYS2 hmg2Δ::HIS3 hrd1Δ::KanMX*
RHY2933	*MATα ade2-101 ura3-52::URA3::HMG2-GFP met2 LYS2 trp1::hisG leu2Δ his3Δ200 hmg2Δ::1MYC-HMG2 hrd1Δ::KanMX*
RHY2936	*Matα ade2-101 ura3-52::URA3::HMG2-GFP met2 lys-801 trp1::hisG leu2Δ his3Δ200::HIS3::pep4Δ hrd1Δ::KanMX ubc7Δ::LEU2*
RHY3005	*MATα ade2-101 ura3-52::URA3::HMGcd::HMG2-GFP met2 lys2-801 trp1::hisG leu2Δ his3Δ200 hmg1Δ::LYS2 hmg2Δ::HIS3 hrd1Δ::KanMX hrd3Δ::LEU2*
RHY4288	*MATα ade2-101 ura3-52 met2 lys2-801 trp1::hisG leu2Δ his3Δ200 HMG1 hmg2Δ::1MYC-HMG2 hrd1Δ::KanMX pep4Δ::HIS3 ubc7Δ::LEU2*
RHY4295	*MATα ade2-101 ura3-52 met2 lys2-801 trp1::hisG leu2Δ his3Δ200 HMG1 hmg2Δ::1MYC-HMG2 hrd1Δ::KanMX pep4Δ::HIS3 ubc7Δ::LEU2 TRP1::TDH3-UBC7-2HA*
RHY5035	*MATα ade2-101 ura3-52::URA3::HMGcd::HMG2-GFP met2 lys2-801 trp1::hisG leu2Δ his3Δ200 hmg1Δ::LYS2 hmg2Δ::HIS3 hrd1Δ::KanMX ubx2Δ::CloNAT*
RHY6152	*MATα ade2-101 ura3-52::HMGcd::HMG2-GFP met2 lys2-801 trp1::hisG leu2Δ his3Δ200 hmg1Δ::LYS2 hmg2Δ::HIS3 hrd1Δ::KanMX URA3::KWW-HA*
RHY6153	*MATα ade2-101 ura3-52::URA3::HMGcd::HMG2-GFP met2 lys2-801 trp1::hisG::TRP1::HRD1-3HA leu2Δ his3Δ200 hmg1Δ::LYS2 hmg2Δ::HIS3 hrd1Δ::KanMX*
RHY6245	*Matα ade2-101 ura3-52::URA3 met2 lys-801 trp1::hisG leu2Δ his3Δ200::HIS3::pep4Δ hrd1Δ::KanMX ubc7Δ::LEU2 TRP1::TDH3-HRD1-3HA*
RHY6374	*MATα ade2-101 ura3-52::URA3::HMGcd::HMG2-GFP met2 lys2-801 trp1::hisG::TRP1::HRD1-3HA S97A S98A D199A leu2Δ his3Δ200 hmg1Δ::LYS2 hmg2Δ::HIS3 hrd1Δ::KanMX*
RHY6459	*MATα ade2-101 ura3-52::HMGcd::HMG2-GFP met2 lys2-801 trp1::hisG leu2Δ his3Δ200 hmg2Δ::HIS3 hrd1Δ::KanMX URA3::CPY*-HA*
RHY6561	*MATα ade2-101 MET2 LYS2 ura3-52 trp1::hisG leu2-3,112 HIS3 hrd1Δ::KanMX sec61-2*
RHY6576	*MATα ade2-101 ura3-52::URA3::HMG2-GFP met2 LYS2 trp1::hisG leu2Δ his3Δ200 hmg2Δ::1MYC-HMG2 hrd1Δ::KanMX HIS3::HA-Pdr5**
RHY7098	*MATα ade2-101 ura3-52::URA3::HMGcd::UPRE4-GFP met2 lys2-801 trp1::hisG leu2Δ his3Δ200 hmg1Δ::LYS2 hmg2Δ::HIS3 hrd1Δ::KanMX*
RHY7099	*MATα ade2-101 ura3-52::URA3::HMGcd::6MYC-HMG2-GFP met2 lys2-801 trp1::hisG leu2Δ his3Δ200 hmg1Δ::LYS2 hmg2Δ::HIS3 hrd1Δ::KanMX*
RHY7510	*MATα ade2-101 ura3-52::HMGcd::HMG2-GFP met2 lys2-801 trp1::hisG leu2Δ his3Δ200 hmg1Δ::LYS2 hmg2Δ::HIS3 hrd1Δ::KanMX URA3::KHN-HA*

RHY7639	*MATα ade2-101 ura3-52::URA3::HMGcd::HMG2-GFP met2 lys2-801 trp1::hisG leu2Δ his3Δ200 hmg1Δ::LYS2 hmg2Δ::HIS3 hrd1Δ::KanMX yos9Δ::CloNAT*
RHY7966	*MATα ade2-101 ura3-52::URA3::HMGcd::HMG2-GFP met2 lys2-801 trp1::hisG leu2Δ his3Δ200 hmg1Δ::LYS2 hmg2Δ::HIS3 hrd1Δ::KanMX yos9Δ::CloNAT LEU2::YOS9-FLAG*
RHY8012	*MATα ade2-101 ura3-52::URA3::HMGcd::HMG2-GFP met2 lys2-801 trp1::hisG leu2Δ his3Δ200 hmg1Δ::LYS2 hmg2Δ::HIS3 hrd1Δ::KanMX usa1Δ::CloNAT*
RHY8015	*MATα ade2-101 ura3-52::URA3::HMGcd::HMG2-GFP met2 lys2-801 trp1::hisG leu2Δ his3Δ200 hmg1Δ::LYS2 hmg2Δ::HIS3 hrd1Δ::KanMX der1Δ::CloNAT*
RHY8022	*MATα ade2-101::ADE2::HRD3-3HA ura3-52::URA3::HMGcd::HMG2-GFP met2 lys2-801 trp1::hisG leu2Δ his3Δ200 hmg1Δ::LYS2 hmg2Δ::HIS3 hrd1Δ::KanMX*
RHY8030	*MATa ADE2 ura3-52 MET2 lys2-801 trp1-1 leu2-3, 112 his3Δ200 UBX2-3HA::KanMX hrd1Δ::CloNAT*
RHY8133	*MATα ade2-101 ura3-52::HMGcd URA3::TDH3-3HA-UBC6 met2 lys2-801 trp1::hisG leu2Δ his3Δ200 hmg1Δ::LYS2 hmg2Δ::HIS3 hrd1Δ::KanMX*
RHY8136	*MATα ade2-101 ura3-52::HMGcd met2 lys2-801 trp1::hisG leu2Δ his3Δ200 hmg1Δ::LYS2 hmg2Δ::HIS3 hrd1Δ::KanMX URA3::STE6-166-3HA-GFP*
RHY8284	*Mata ADE2 ura3-52 MET2 lys2-801 trp1-1::TRP1::USA1-6xHA leu2-3,112 his3Δ200 HMG1 HMG2 hrd1Δ::CloNAT*

Table S3. Strains used in this study with the corresponding figure

Parent Strain	Plasmid Expressed	Figure
RHY2814	pRH507	6B, 6C, S5B, S5C
	pRH642	2A, 3A, 3B, 3D, 3E, 4F, 5B, 5D, 5H, 6A, 6D, S3B, S3D, S4C, S4D, S5A, S5D
	pRH730	3E
	pRH1245	3B, 3D, 3E, 5B, 5D, 5H, S3B, S3D, S4D
	pRH1718	3E
	pRH2213	3A
	pRH2248	3A
	pRH2269	3A, 3B, 3D, 3E, 4F, 6A, 6D, S5A, S5D
	pRH2288	6B, 6C, S5B, S5C
	pRH2316	5H, S4C, S4D
	pRH2344	2A
	pRH2345	2A
	pRH2350	2A
	pRH2352	5B, S3B
	pRH2360	5D, S3D
	pRH2365	3E
RHY2933	pRH642	7A
	pRH2269	7A
RHY2936	pRH730	7B, 7C, S6
	pRH808	7C
	pRH1718	S6
	pRH2365	7B, 7C, S6
	pRH2366	7C
	pRH2517	S6
RHY3005	pRH311	6E
	pRH642	4F, 6E, S1, S3G
	pRH730	6E
	pRH1245	S1
	pRH2269	4F, S1
	pRH2287	S1
	pRH2360	S3G
	pRH2365	6E
RHY4288		7C
RHY4295		7C
RHY5035	pRH507	6C, S5C
	pRH2288	6C, S5C

RHY6152	pRH311 pRH507 pRH2288 pRH2361 pRH2362 pRH2364	2E, 4C 2E, 4C 4C 2E 2E 2E
RHY6153	pRH311 pRH2078	6J 6J
RHY6245		7B
RHY6374	pRH2078	6J
RHY6459	pRH311 pRH507 pRH2288 pRH2361 pRH2362 pRH2364 pRH2398	2D, 4A, S3F 2D, 4A, S3F 4A 2D 2D 2D S3F
RHY6561	pRH642 pRH1245 pRH2269 pRH2316 pRH2360	4E, 5E, 5F, S3E, S4A 4E, 5E, 5F, S3E, S4A 4E 5F, S4A 5E, S3E
RHY6576	pRH642 pRH1245 pRH2269 pRH2316 pRH2344 pRH2345 pRH2350 pRH2352 pRH2360	2C, 4D, 5A, 5C, 5G, S3A, S3C, S4B, S4E 4D, 5A, 5C, 5G, S3A, S3C, S4B, S4E 4D 5G, S4B, S4E 2C 2C 2C 5A, S3A 5C, S3C
RHY7098	pRH642 pRH1245 pRH2269	S2 S2 S2
RHY7099	pRH642 pRH1245 pRH2269 pRH2344 pRH2345 pRH2350	2B, 3C 3C 3C 2B 2B 2B
RHY7510	pRH311 pRH507 pRH2288	4B 4B 4B
RHY7639	pRH642 pRH2269	6A, S5A 6A, S5A

RHY7966	pRH311 pRH642 pRH2269	6F 6F 6F
RHY8012	pRH507 pRH2288	6B, S5B 6B, S5B
RHY8015	pRH642 pRH2269	6D, S5D 6D, S5D
RHY8022	pRH311 pRH642 pRH2269	6G 6G 6G
RHY8030	pRH311 pRH642 pRH2269	6H 6H 6H
RHY8133	pRH311 pRH642	6K 6K
RHY8136	pRH311 pRH642	6L 6L
RHY8284 x RHY2933	pRH311 pRH642 pRH2269	6I 6I 6I

Supplemental Experimental Procedures

DNA manipulation and plasmid construction

Hrd1p mutants were generated with the splicing by overlap elongation (SOEing) PCR technique (Horton et al., 1989). Oligo nucleotide sequences used for PCR are available upon request. The KWW and KHN plasmids were a generous gift from D. Ng (National University of Singapore). The Pdr5* plasmid (pRH2312) was a generous gift from D. Wolf (University of Stuttgart). The Yos9p-Flag plasmid was a generous gift from J. Weissman (University of California, San Francisco).

Yeast and Bacterial strains

The LiOAc method was utilized to transform yeast strains with plasmid DNA (Ito et al., 1983). Null alleles were constructed by transforming yeast with the LiOAc method with a PCR product that encoded either G418 resistance or CloNAT/nourseothricin (Werner BioAgents, Jena, Germany) resistance and contained 50bp flanks homologous to the gene to be knocked out. (Baudin et al., 1993). Cells were allowed to grow on yeast peptone dextrose (YPD) for ~12 hours and were then replica plated onto YPD plus 500μg/ml G418 or 200 μg/ml nourseothricin. The UBX2-3HA containing strain was a generous gift from A. Buchberger (Max Planck Institute of Biochemistry). The USA1-6HA strain was a generous gift from T. Sommer (Max-Delbruck Center for Molecular Medicine).

Degradation assays and UPR measurements

For cycloheximide chases, cells were incubated with 50μg/ml cycloheximide and identical amounts were removed at the given time points. Cells were incubated with SUME lysis buffer (1% SDS, 8M Urea, 10mM MOPS pH 6.8, 10mM EDTA) and were lysed by vortexing for 3 minutes. An equal volume of 2X urea sample buffer (75mM MOPS pH 6.8, 4% SDS, 200mM DTT, 0.2mg/ml bromophenol blue, 8M urea) was then added. Samples were analyzed by SDS-PAGE and immunoblotting. Total protein levels in each lane were equal as was verified by India ink staining (data not shown). Flow cytometry was undertaken as described (Sato and Hampton, 2006). Cells were grown to log phase and cycloheximide was added. All samples were processed at the same time. Data was obtained through a FACScalibur machine (Becton, Dickinson and Company, Franklin Lakes, NJ) and statistical analysis was performed with CellQuest software (Becton, Dickinson and Company, Franklin Lakes, NJ). The Sec61 antibody used to study Sec61-2p degradation was a generous gift from R. Schekman (University of California, Berkeley).

Ubiquitination assay

Cells were incubated with 10μg/ml zaragozic acid or a DMSO control for 7 minutes. Following this treatment, 3 OD of cells were pelleted. 100μl of SUME with protease inhibitors and N-ethyl maleimide (NEM) and 100μl of glass beads were added to lyse the cells. 1ml of IP buffer (150mM NaCl, 15mM Na_2HPO_4, 2% Triton-X100, 0.1% SDS, 0.5% DOC, 10mM EDTA, pH 7.5) with protease inhibitors and NEM was added to the cell extracts and the mix was centrifuged for 5 minutes at 14,000 x g. The supernatant was removed and 15μl of polyclonal

anti-GFP antibody was added. The mix was incubated overnight at 4°C. 100µl of Protein-A Sepharose (Amersham Biosciences) in IP buffer, (50% w/v) was added for 2 hours. Beads were washed once with IP buffer and once with IP wash buffer (50mM NaCl, 10mM Tris, pH 7.5) and incubated with 50µl of 2x Urea sample buffer for 10 minutes at 50°C. The samples were then loaded on a polyacrylamide gel. Following transfer to nitrocellulose, immunoblotting with an anti-ubiquitin or anti-GFP antibody was performed.

Cross-linking assay

Cells were grown to log phase, harvested and resuspended in B88 buffer (20mM Hepes pH6.8, 250mM sorbitol, 150mM KOAc, 5mM MgOAc) plus protease inhibitors. Microsomes were prepared by vortexing for 6 minutes (1 minute vortex, 1 minute on ice) and spun down at 21,000 x g for 30 minutes. Microsomes were then resuspended and incubated with either DMSO or increasing concentrations of DSP (Pierce Biotechnology, Rockford, IL) for 40 minutes at room temperature. Tris pH7.5 was then added to a final concentration of 50mM for 10 minutes after which the microsomes were centrifuged again. Microsomes were then lysed in 300µl SUME lysis buffer plus 1% Triton-X100 and 0.5% DOC. 1ml IP buffer was added to each tube along with 15µl of anti-GFP antibody and incubated overnight at 4°C. The antibody was bound to Protein-A Sepharose beads for 2 hours and the beads were washed with IP buffer and IP wash buffer. The beads were then incubated with 50µl of 2x Urea sample buffer for 10 minutes at 50°C.

Native co-immunoprecipitation

Microsomes were harvested as previously described in MF buffer (20mM Tris pH7, 100mM NaCl, 300mM sorbitol). Once centrifuged, microsomes were resuspended in 1ml of Tween IP buffer (500mM NaCl, 50mM Tris pH7.5, 100mM EDTA, 1.5% Tween-20) and incubated on ice for 15 minutes. Lysates were then centrifuged for 30 minutes at 14,000 x g and the supernatant was incubated with 15µl of anti-GFP or anti-Hrd1p antibody overnight at 4°C followed by 2 hours with Protein-A Sepharose beads. For the Cdc48 co-IP, Cdc48 was immunoprecipitated with IgG-Sepharose beads for 2 hours at 4°C. The beads were then washed with the Tween-20 IP buffer and incubated with 50µl of 2x Urea sample buffer for 10 minutes at 50°C.

Dilution Assays

Cells were grown to log phase and 0.35 OD units (ABS = 600nm) were harvested for each strain. Five-fold dilutions were then performed at the serially diluted cultures were spotted on synthetic complete media lacking the appropriate supplements. Plates were incubated at the indicated temperatures for three days.

Supplemental Figures

Figure S1

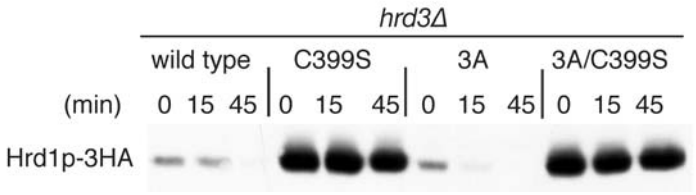

Figure S2

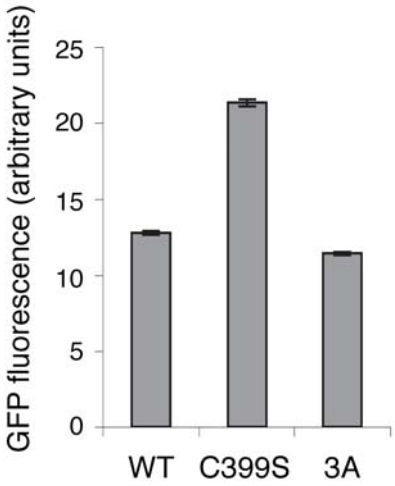

Figure S3

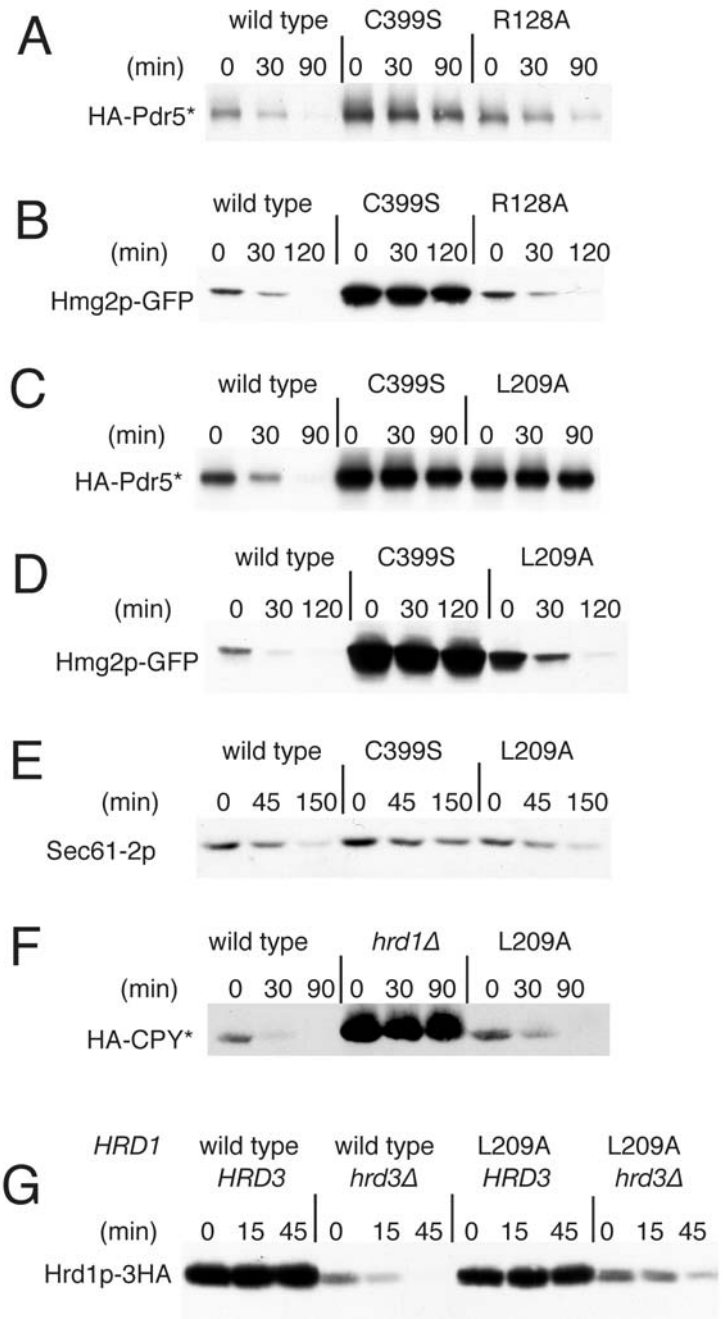
A
wild type
C399S
R128A
(min)
0 30 90 0 30 90 0 30 90
HA-Pdr5*
B
wild type
C399S
R128A
(min)
0 30 120 0 30 120 0 30 120
Hmg2p-GFP
C
wild type
C399S
L209A
(min)
0 30 90 0 30 90 0 30 90
HA-Pdr5*
D
wild type
C399S
L209A
(min)
0 30 120 0 30 120 0 30 120
Hmg2p-GFP
E
wild type
C399S
L209A
(min)
0 45 150 0 45 150 0 45 150
Sec61-2p
F
wild type
hrd1Δ
L209A
(min)
0 30 90 0 30 90 0 30 90
HA-CPY*
G
HRD1
wild type
HRD3
wild type
hrd3Δ
L209A
HRD3
L209A
hrd3Δ
(min)
0 15 45 0 15 45 0 15 45 0 15 45
Hrd1p-3HA

Figure S4

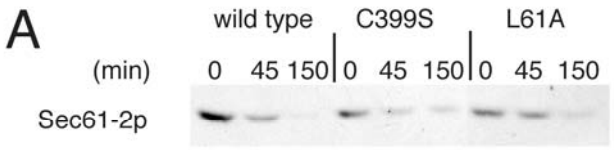
A
wild type
C399S
L61A
(min)
0 45 150 0 45 150 0 45 150
Sec61-2p


B
wild type
C399S
L61A
(min)
0 30 90 0 30 90 0 30 90
HA-Pdr5*

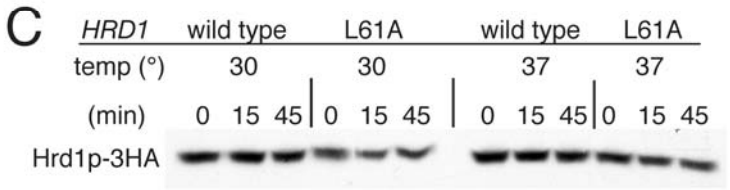
C
HRD1
wild type
L61A
wild type
L61A
temp (°)
30
30
37
37
(min)
0 15 45 0 15 45 0 15 45 0 15 45
Hrd1p-3HA

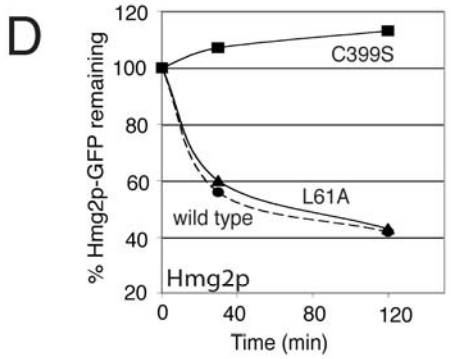
D
% Hmg2p-GFP remaining
120
100
80
60
40
20
C399S
L61A
wild type
Hmg2p
0
40
80
120
Time (min)

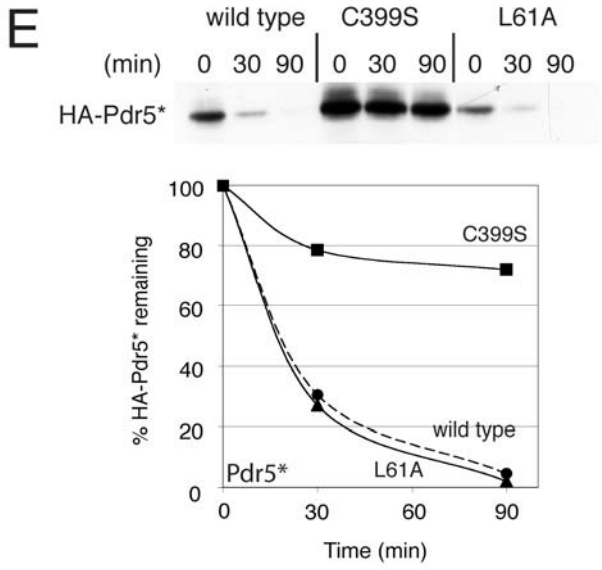
E
wild type
C399S
L61A
(min)
0 30 90 0 30 90 0 30 90
HA-Pdr5*
% HA-Pdr5* remaining
100
80
60
40
20
0
C399S
wild type
Pdr5*
L61A
0
30
60
90
Time (min)

Figure S5

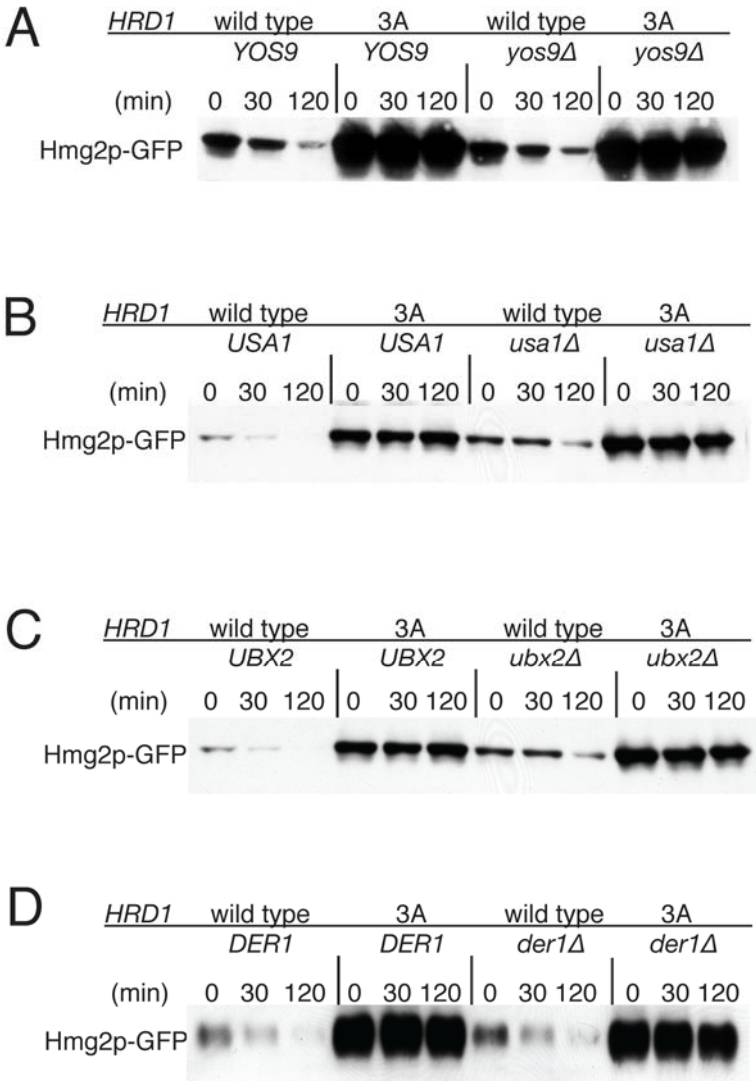
A
HRD1
wild type
3A
wild type
3A
YOS9
YOS9
yos9Δ
yos9Δ
(min)
0 30 120 0 30 120 0 30 120 0 30 120
Hmg2p-GFP
B
HRD1
wild type
3A
wild type
3A
USA1
USA1
usa1Δ
usa1Δ
(min)
0 30 120 0 30 120 0 30 120 0 30 120
Hmg2p-GFP
C
HRD1
wild type
3A
wild type
3A
UBX2
UBX2
ubx2Δ
ubx2Δ
(min)
0 30 120 0 30 120 0 30 120 0 30 120
Hmg2p-GFP
D
HRD1
wild type
3A
wild type
3A
DER1
DER1
der1Δ
der1Δ
(min)
0 30 120 0 30 120 0 30 120 0 30 120
Hmg2p-GFP

Figure S6

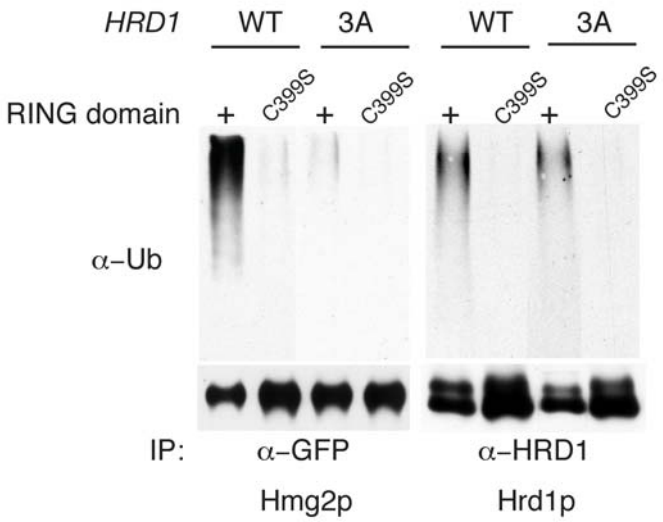
HRD1
WT
3A
WT
3A
RING domain
+
C399S
+
C399S
+
C399S
+
C399S
α–Ub
IP:
α–GFP
α–HRD1
Hmg2p
Hrd1p

Figure S7

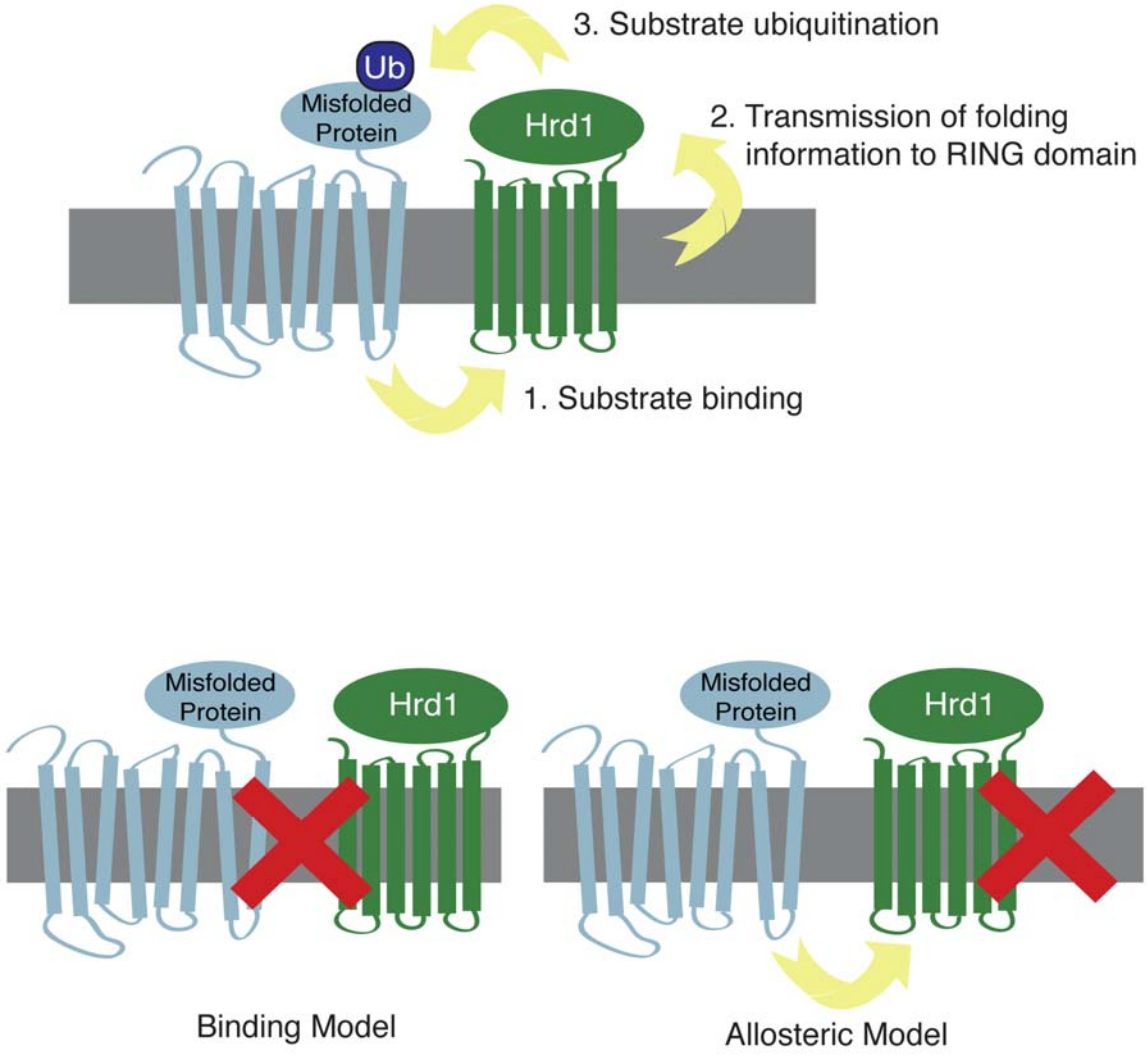
3. Substrate ubiquitination
Ub
Misfolded Protein
Hrd1
2. Transmission of folding information to RING domain
1. Substrate binding
Misfolded Protein
Hrd1
Binding Model
Misfolded Protein
Hrd1
Allosteric Model

Supplemental Figure Legends

Figure S1

3A-Hrd1p underwent self-degradation in a C399S dependent manner. Hrd1p self-degradation was tested by cycloheximide chase of isogenic *hrd1*Δ*hrd3*Δ strains expressing the indicated Hrd1p proteins. Cycloheximide chases were performed as described in Figure 2.

Figure S2

A strain expressing 3A-Hrd1p did not upregulate UPR. Strains expressing the UPRE4-GFP reporter and the indicated versions of Hrd1p were grown to log phase and the GFP fluorescence was measured by flow cytometry. Each bar represents 10,000 cells analyzed and the standard error of the mean is noted.

Figure S3

R128A and L209A Hrd1p are impaired in Pdr5* degradation. (A-E) Cycloheximide chases were performed on strains expressing the given Hrd1p and degradation substrate as described in Figure 2. Statistics for the western blots can be found in Figure 5A-E. (F) A cycloheximide chase utilizing strains expressing the indicated version of Hrd1p and the ERAD-L substrate CPY* was performed as described. (G) Isogenic *hrd1*Δ or *hrd1*Δ*hrd3*Δ strains transformed with the indicated *HRD1* were utilized to examine Hrd1p self-degradation.

Figure S4

L61A Hrd1p is impaired in Sec61-2p degradation but proficient at degrading other ERAD-M substrates. (A, B) Cycloheximide chases were performed on strains expressing the given Hrd1p and degradation substrate as described in Figure 2. Statistics for the western blots can be found in Figure 5F, 5G. (C) L61A Hrd1p stability was analyzed at 30°C and 37°C by cycloheximide chase. Prior to the addition of cycloheximide, cells were pre-incubated at the indicated temperature for 15 minutes. (D-E) Degradation of the indicated protein was analyzed in strains expressing wild type, C399S, or L61A Hrd1p at 37°C. Prior to the addition of cycloheximide, cells were pre-incubated at 37°C for 15 minutes.

Figure S5

The role of other ERAD factors in Hmg2p-GFP degradation is unaltered by 3A-Hrd1p. (A-D) Cycloheximide chases were performed to examine Hmg2p-GFP degradation as described in Figure 2. Degradation was assayed in the absence of the indicated ERAD factor. Statistics for the experiments are shown in Figure 6.

Figure S6

In vitro ubiquitination was dependent on a functional Hrd1 RING domain. Microsomes and cytosol were harvested from strains expressing the indicated proteins and utilized for an *in vitro* ubiquitination assay as described in Figure 7. Anti-GFP or anti-Hrd1 immunoprecipitations were performed and the resulting pull-down was analyzed by immunoblotting.

Figure S7

An allosteric model for Hrd1p-dependent ubiquitination of a misfolded membrane protein. Hrd1p binding to a misfolded protein is not sufficient to catalyze ubiquitination. It appears that, following binding, the transmembrane domain must relay structural information about the misfolded protein to Hrd1p's RING domain, after which substrate ubiquitination can occur.